AD-A125 510 THE GENERATION OF NEAR MILLIMETER RADIATION BY PICOSECOND PULSE DEMODULATION(U) DUKE UNIV DURHAM NC DEPT OF PHYSICS F C DE LUCIA JAN 83 DAAK70-79-C-0121 1/1

UNCLASSIFIED F/G 17/9 NL

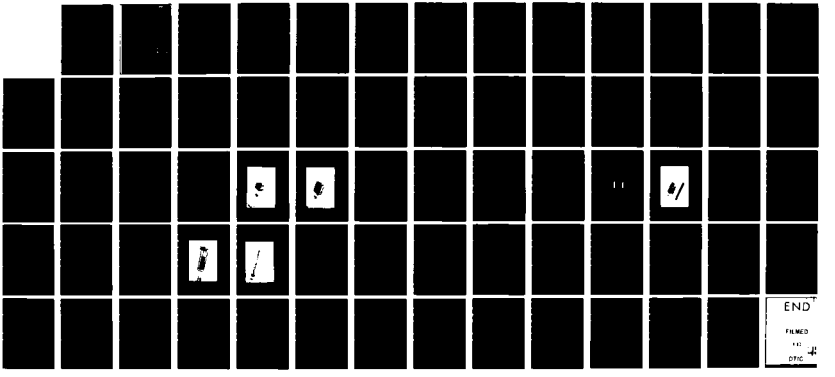

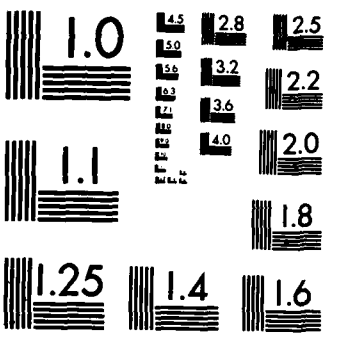

MICROCOPY RESOLUTION TEST CHART
NATIONAL BUREAU OF STANDARDS-1963-A

FINAL REPORT

to

THE NIGHT VISION AND ELECTRO-OPTICS LABORATORY

by

Department of Physics, Duke University
Durham, North Carolina 27706

THE GENERATION OF NEAR MILLIMETER RADIATION BY PICOSECOND PULSE DEMODULATION

January 1983

UNCLASSIFIED

SECURITY CLASSIFICATION OF THIS PAGE (When Data Entered)

REPORT DOCUMENTATION PAGE		READ INSTRUCTIONS BEFORE COMPLETING FORM
1 REPORT NUMBER	2 GOVT ACCESSION NO	3 RECIPIENT'S CATALOG NUMBER
4. TITLE (and Subtitle) THE GENERATION OF NEAR MILLIMETER RADIATION BY PICOSECOND PULSE DEMODULATION		5 TYPE OF REPORT & PERIOD COVERED FINAL SCIENTIFIC REPORT 8/1/79 - 10/1/82 6. PERFORMING ORG REPORT NUMBER
7. AUTHOR(s) Frank C. De Lucia		8. CONTRACT OR GRANT NUMBER(s) DAAK 70-79-C-0121
9 PERFORMING ORGANIZATION NAME AND ADDRESS Duke University Durham, North Carolina 27706		10 PROGRAM ELEMENT PROJECT TASK AREA & WORK UNIT NUMBERS
11 CONTROLLING OFFICE NAME AND ADDRESS Night Vision and Electro-Optics Laboratory Fort Belvoir, Virginia 22060		12 REPORT DATE January 1983 13 NUMBER OF PAGES 59
14. MONITORING AGENCY NAME AND ADDRESS (if different from Controlling Office)		15. SECURITY CLASS (of this report) UNCLASSIFIED 15a DECLASSIFICATION/DOWNGRADING SCHEDULE
16. DISTRIBUTION STATEMENT (of this Report) Approved for public release; distribution unlimited		
17. DISTRIBUTION STATEMENT (of the abstract entered in Block 20, if different from Report)		
18. SUPPLEMENTARY NOTES Mr. Byong Ahn was the contract monitor for this project.		
19. KEY WORDS (Continue on reverse side if necessary and identify by block number)		

20 ABSTRACT (Continue on reverse side if necessary and identify by block number) Near Millimeter Waves can be generated by the demodulation of a picosecond optical pulse train by a photocathode. Power is produced by the interaction of a microwave structure and the beam of prebunched electrons produced by the demodulation. These bunched electrons are produced at a photocathode by a picosecond optical pulse train. The separation of the bunching process from the energy extraction interaction introduces substantial flexibility into the design of devices based upon this concept. Perhaps the most important manifestation of this flexibility is the capability of these devices to

DD FORM 1 JAN 73 1473 EDITION OF 1 NOV 65 IS OBSOLETE

UNCLASSIFIED

SECURITY CLASSIFICATION OF THIS PAGE (When Data Entered)

[20] continued:

to provide virtually any waveform and pulse sequence desired with complete pulse to pulse phase coherence and rapid, controlled frequency agility. Furthermore, techniques are discussed that can change this coding at speeds governed only by electrooptic time scales. It is also important to note that these devices are not quantum down convertors (which would be limited by Manley-Rowe considerations to a maximum efficiency of ~0.1%) but rather "classical" devices in which gain phenomena can convert DC power to microwave energy, thus providing orders of magnitude more efficiency. In this report and its appendixes, we discuss the basic physics of picosecond demodulation devices, experimental results and systems based upon these concepts.

FOREWORD

This report was prepared by the Physics Department of Duke University. This work was sponsored by the Night Vision and Electro-Optics Laboratory under contract No. DAAK 70-79-C-0121.

The report covers work performed between 1 August 1979 and 1 October 1982. The contract monitor was Mr. Byong Ahn, Laser Division, Night Vision and Electro-Optics Laboratory, Fort Belvoir, Virginia, 22060. The principal investigator was Frank C. De Lucia. Additional work was performed by P. Wheless, R. McMahon, and A. Charo.

TABLE OF CONTENTS

LIST OF FIGURES

LIST OF FIGURES

ABSTRACT

Near Millimeter Waves can be generated by the demodulation of a picosecond optical pulse train by a photocathode. Power is produced by the interaction of a microwave structure and the beam of prebunched electrons produced by the demodulation. These bunched electrons are produced at a photocathode by a picosecond optical pulse train. The separation of the bunching process from the energy extraction interaction introduces substantial flexibility into the design of devices based upon this concept. Perhaps the most important manifestation of this flexibility is the capability of these devices to provide virtually any waveform and pulse sequence desired with complete pulse to pulse phase coherence and rapid, controlled frequency agility. Furthermore, techniques are discussed that can change this coding at speeds governed only by electrooptic time scales. It is also important to note that these devices are not quantum down convertors (which would be limited by Manley-Rowe considerations to a maximum efficiency of ~0.1%) but rather "classical" devices in which gain phenomena can convert DC power to microwave energy, thus providing orders of magnitude more efficiency. In this report and its appendixes, we discuss the basic physics of picosecond demodulation devices, experimental results and systems based upon these concepts.

I. INTRODUCTION

The production and detection of electromagnetic radiation in the Near Millimeter spectral region has been a scientific and technological challenge for over thirty years. Among the potential uses of such a technology are high resolution, small aperture radar capable of penetrating dust and fog; the diagnostic study of quantum electronic devices; and a host of laboratory and spectroscopic studies.

This report contains the results of an experimental study of picosecond demodulation devices as sources of Near Millimeter Wave Radiation. Included are discussions of the basic physics and attributes of these devices, description of experimental devices that have been constructed and experimental results achieved, and discussions of possible systems that could utilize this concept.

II. BASIC PHYSICS AND CONFIGURATIONS OF PICOSECOND DEMODULATION SOURCES.

Conceptually the simplest configuration is based upon the photoemission of electrons and is shown in Figure 1. This particular device would be very inefficient and is used only to illustrate the concept. The picosecond pulse train causes electrons to be ejected at low energy (~1 eV) from the photocathode and these electrons are subsequently accelerated by V_o across the waveguide. The interaction of these bunched electrons with the microwave structure is fundamentally very similar to the interaction between an electron beam that has been bunched by velocity modulation and the resonant mode structure of a klystron. Consequently, the ultimate characteristics of picosecond demodulation devices will be strongly related to the characteristics of other electron beam devices (e.g. travelling wave tubes, extended interaction oscillators, free electron lasers, etc.) For example, picosecond demodulation devices are not quantum down converters with a correspondingly small efficiences (<.1%). On the contrary, they are semi-classical devices with the capability of substantially more power output than optical power input.

One of the principal attributes of picosecond demodulation sources is their ability to generate, via straight forward optical control, a wide variety of complex waveforms with frequency agility and pulse to pulse phase coherence. First let us consider the very simple optical pulse train shown in Figure 2.

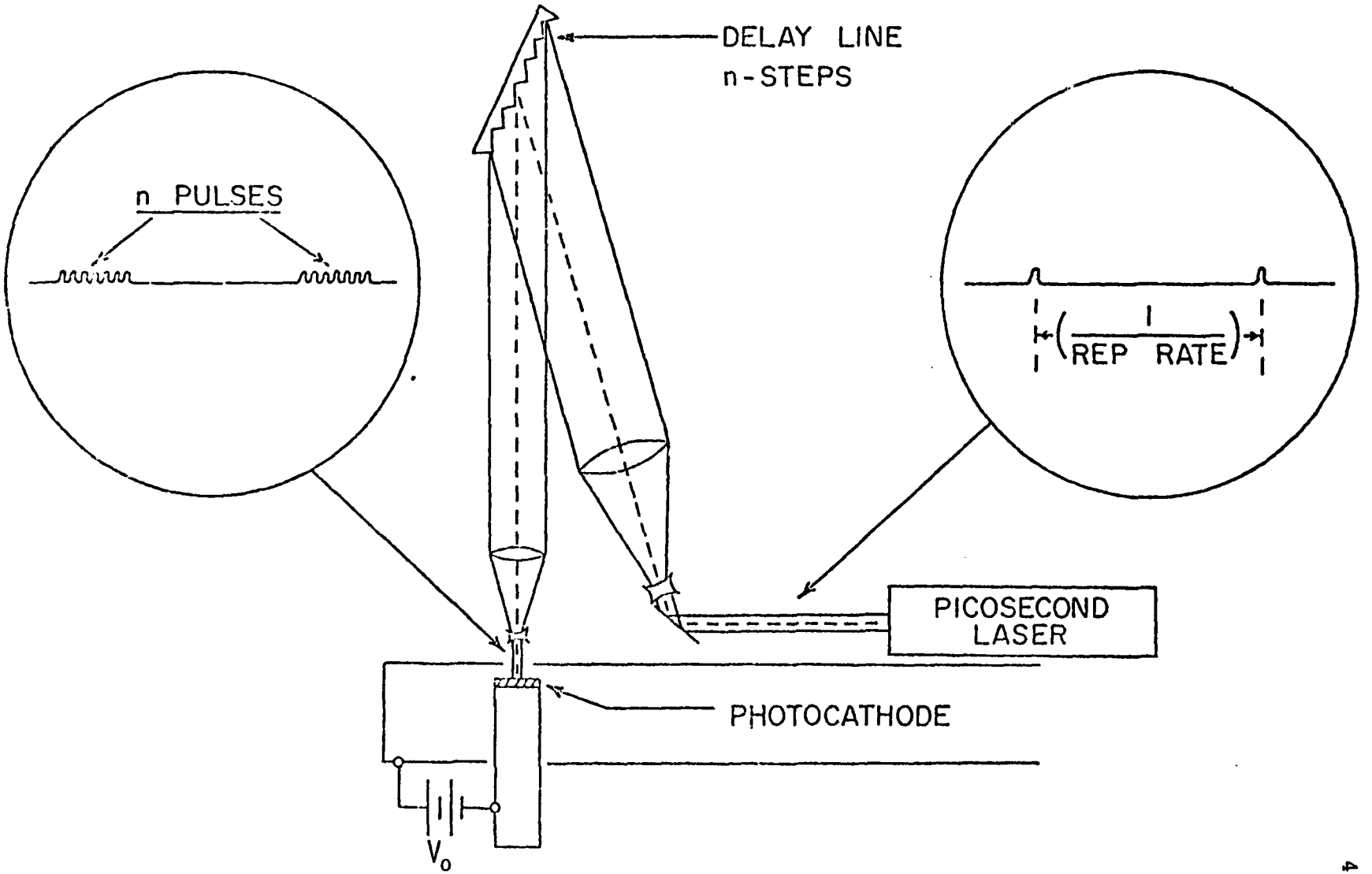

FIGURE 1. A SIMPLE PICOSECOND DEMODULATION NMMW SOURCE.

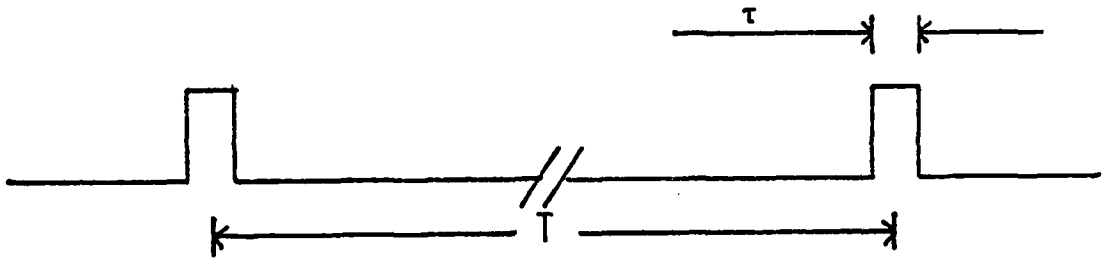

FIGURE 2. THE OPTICAL PULSE TRAIN FROM A MODE-LOCKED PICOSECOND LASER.

Microwave sources based upon this type of optical pulse train have several interesting properties. Conceptually the picosecond demodulation is the inverse of the laser mode locking that produced the picosecond optical pulses. A mode locked laser is simply one running on many phase related modes simultaneously. Figure 3 shows such a spectrum for a laser of N modes, centered on ω_o

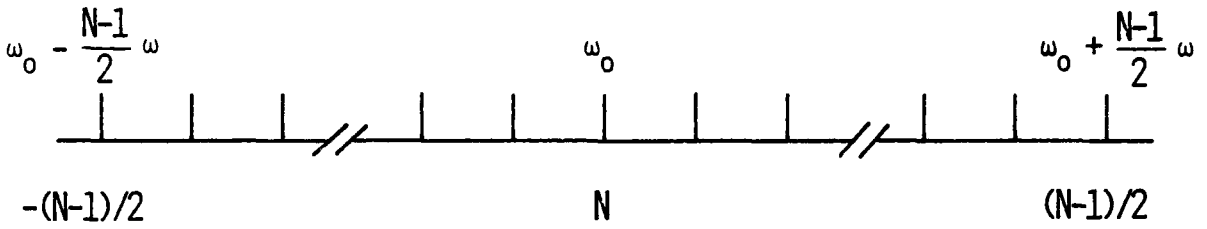

FIGURE 3. SPECTRUM OF A MODE-LOCKED LASER.

If each mode has electric field E_o, the total laser field is

$$E(t) = E_o \sum_{-(N-1)/2}^{(N-1)/2} e^{i(\omega_o + n\omega)t} = E_o e^{i\omega_o t} \frac{\sin(N\omega/2)}{\sin(\omega t/2)} \qquad (1)$$

The laser power output is then proportional to

$$\frac{\sin^2(N\omega t/2)}{\sin^2(\omega t/2)} \qquad (2)$$

This relations leads to the following conclusions about mode locked lasers:

1. The power is emitted as a train of pulses of period $T=2\pi/\omega$
2. The peak power is N times the average power
3. The individual pulse width $\tau=T/N=2\pi/N\omega=1/$(bandwidth of modes locked together)

If such a pulse train is used to drive a picosecond demodulation source, the lattice spacing of the microwave signals is $\Delta\nu=\omega/2\pi$ and the frequencies produced, $\nu_n=n\omega/2\pi$. Now if a microwave structure will support the same number of components, N, that were supported by the laser, the microwave source has the same picosecond characteristics as the drive laser and Figures 2 and 3 are also representative of the microwave source. Put another way, if one of the components n is looked at individually, it is simply a cw microwave source; on the other hand if all N of the n components are coupled out, then the mathematics of Eqs. 1 and 2 apply and the microwave source is a picosecond source with a repetition rate of $T=\frac{2\pi}{\omega}$. It is important to note that microwave pulses of length <<1 nanosecond can be produced this way.

Now let us discuss the production of generalized waveforms. We will initially assume that we have a single picosecond pulse of energy to divide by optical means. Let us first consider a specific example, shown in Figure 4. By adjusting the spacing and width of the steps in the mirror, the pulse timing and amplitude are completely adjustable over the maximum delay range [2 x depth of mirror/c]. Even this limit is easily circumvented by slightly more complex multiple reflection configurations. Examples of waveforms are shown in the figure. Since it is possible to use cylindrical optics to produce a flat beam, many different pulse sequences can be stored on a single encoder vertically and each selected by a simple vertical translation of either the flat beam or the mirror.

For faster switching and also to allow for an almost infinite number of pulse sequences, each of the reflector steps could be

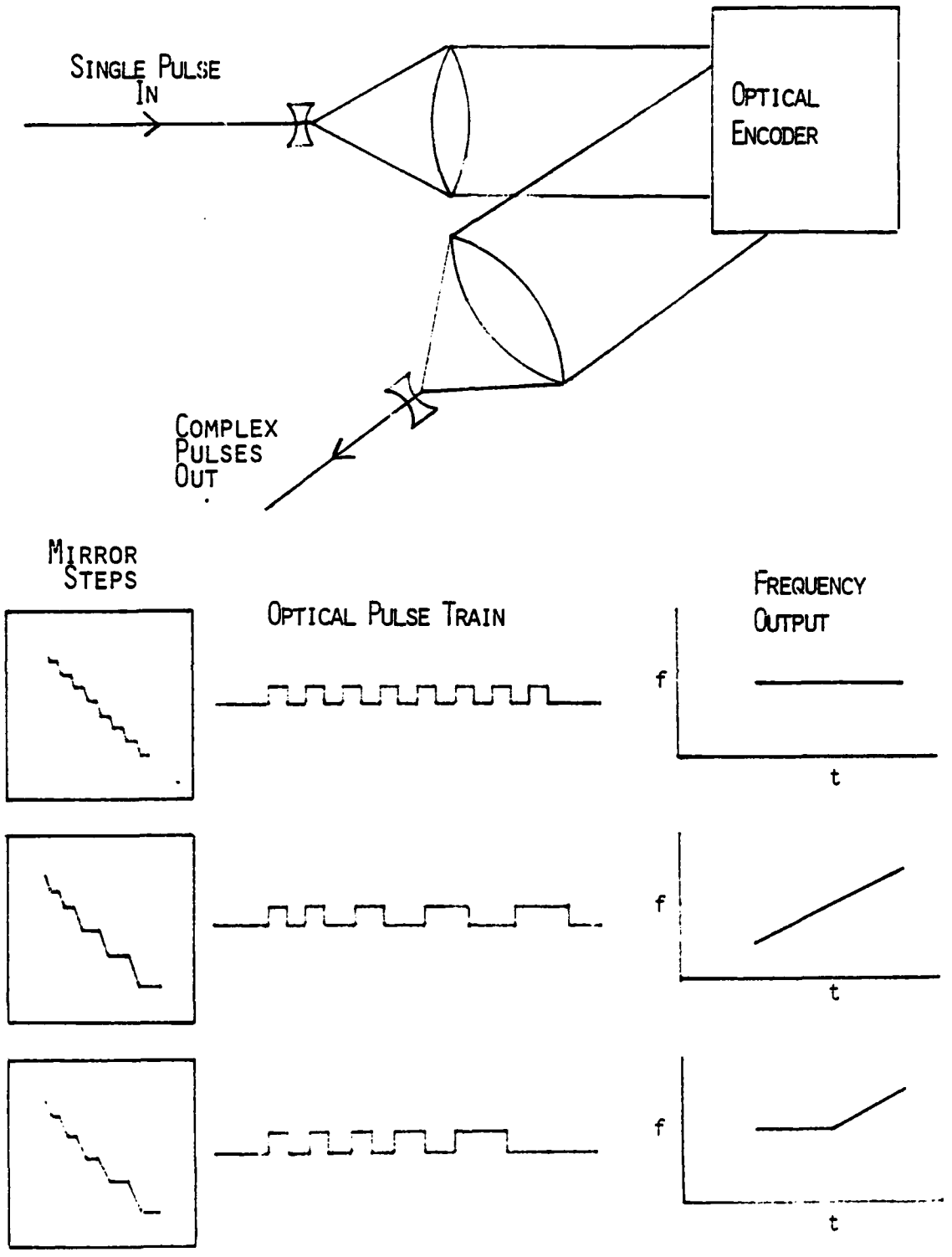

FIGURE 4. GENERATION OF COMPLEX WAVEFORMS IN PICOSECOND DEMODULATION SOURCES.

individually addressable via electrooptic techniques. Thus we conclude that a wide variety of rapidly switchable, phase coherent waveforms (the phase is directly relatable to the phase of the mode locker) are readily generated.

Now let us investigate the power produced by picosecond demodulation sources and the parameters upon which this power depends. Let us first consider the microwave spectrum that is produced by the repetitive current pulse train, shown in Figure 5. This current train results from the optical pulse train of Figure 2 and can serve as the basis for calculating the microwave power produced by more complex pulse sequences.

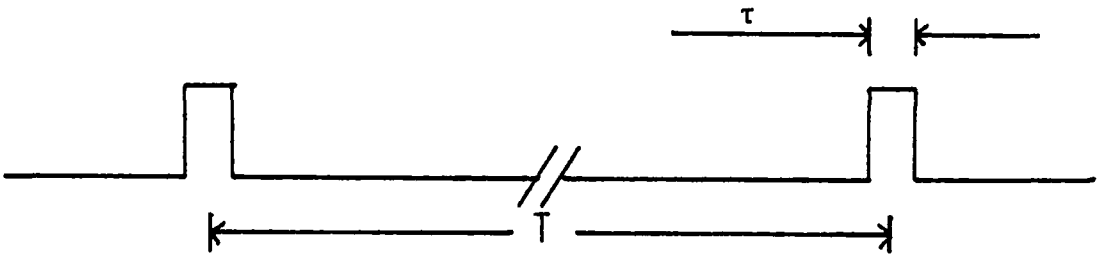

FIGURE 5. ONE CYCLE OF A REPETITIVE CURRENT PULSE TRAIN.

The Fourier components of this pulse train are

$$f(t) = \frac{\tau}{T} + \frac{2}{\pi} \sum_{n=1}^{\infty} \frac{(-1)^n}{n} \sin \frac{n\pi\tau}{T} \cos \frac{n2\pi t}{T} \quad . \tag{3}$$

In the limit $\tau/T<<1$ (i.e. the width of the picosecond pulse is very small in comparison to the time between pulses)

$$f(t) = \frac{\tau}{T} + \frac{2}{\pi} \sum_{n=1}^{\infty} (-1)^n \pi\frac{\tau}{T} \cos \frac{2\pi nt}{T} \tag{4}$$

and each frequency component is given by

$$f(t)_n = 2\frac{\tau}{T} \cos \frac{n2\pi t}{T} \quad . \tag{5}$$

Since at a photocathode, the current produced is proportional to the optical power, we can write

$$i(t)_n = i_n \cos \frac{n2\pi t}{T} = 2i_a \cos \frac{n2\pi t}{T} \quad . \tag{6}$$

where i_n is the current in the $n^{\underline{th}}$ component and i_a is the average current. In the Appendix we develop the relation between the pulsed photocurrent and the resultant microwave power to be $P=i^2R'$ where i is the current in a modulated current beam and R' is the coupling impedance of the microwave structure (including transit time effects). Thus for the waveform of Figure 5, we have

$$P_n = (2i_a)^2 R'_n \quad . \tag{7}$$

It should be noted that in the delta function current pulse limit, this spectrum extends to $n = \infty$. However, conservation of energy is not violated even in this ideal case because the derivation in the Appendix does not include the deceleration of the electron beam by the microwave field. Thus we reach our first important scaling law result, that the microwave power produced is related to the square of the optical power that drives the photocathode.

Now let us consider the result of redistributing available optical puse power among different forms of pulse trains. Assume that we take the pulse train of Figure 5, keep the average power the same, but redistribute the energy to make many smaller pulses separated in time by $1/\nu_{MW}$ where ν_{MW} is the frequency we wish to generate (this is the cw limit). Since the average power remains

the same, Eq. (7) gives us the same power per component, but now there is only one component. This change has the following implications:

1. We now have a single cw component, rather than many phase related components which produced the pulse structure.
2. The total microwave output power has been reduced by a factor equal to the original number of components.
3. We will show later that we can now use high Q resonant circuits to increase R by as much as x100 when we have one or only a few components.

Now let us consider a different kind of pulse train shown in Figure 6. This pulse train is typical of higher power, but lower repetition rate solid state lasers. Assume that the laser produces a pulse train of n pulses (n~10) of width τ, separated by a period T (~10^{-8} sec). Again, by use of

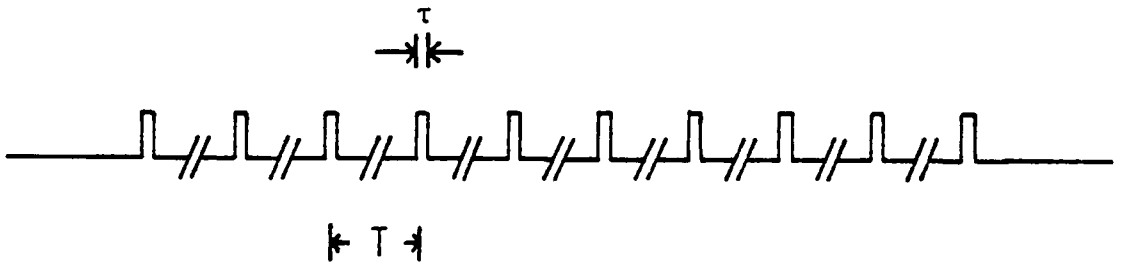

FIGURE 6. PULSE TRAIN FROM A "PULSED" PICOSECOND LASER.

optical delay line techniques we could redistribute this energy among many small pulses ($n\frac{T}{t}$) or leave it in its original form with the same implications as above. As long as n ≥10, the fact that the pulse train ends (we are now driving it with a "pulsed" mode locked laser rather than a "cw" mode locked laser) does not effect any of

the conclusions above. It simply means that we are producing a pulsed rather than cw microwave source (of course both microwave sources still have a picosecond pulse substructure because of the mode locking effects discussed above).

Stated more specifically, if one drives a picosecond demodulation source with the wave form below

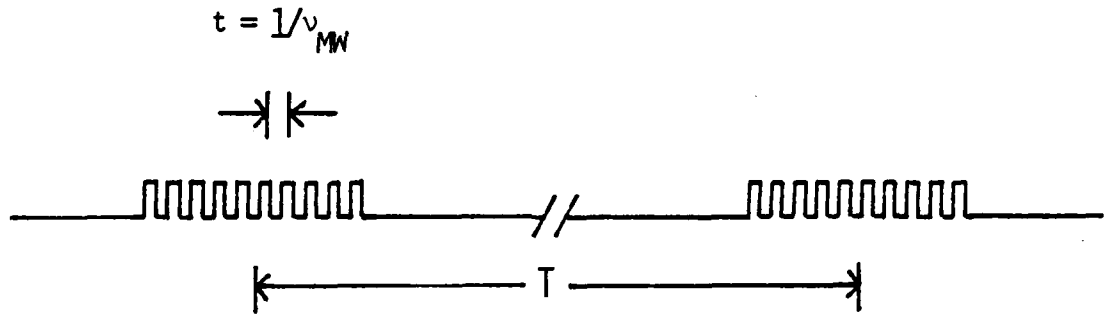

FIGURE 7. PULSE TRAIN FROM THE PHOTOCATHODE FOR A PULSED MICROWAVE SOURCE.

we produce primarily a single microwave component of frequency ν_{MW} whose peak power is greater by (1/duty cycle)^2 and whose average power is greater by (1/duty cycle) than a cw microwave source. This type of source is similar to a conventional radar source. If driven by an actively mode locked laser, the microwave signal will have pulse-to-pulse phase coherence. With an active mode locker, the microwave frequency is always phase related (in fact a harmonic) of the mode locker frequency. Thus the picosecond demodulation source produces microwave pusles which have pulse to pulse phase coherence. On the other hand, if passive mode locking is used, the pulse-to-pulse phase coherence is lost.

Thus we reach our second important conclusion; in the limit that the system is laser power limited, the duty cycle chosen is an important parameter in determing not only the peak power output, but also the average power output of the system.

Equation 7 would seem to imply that the voltage used to accelerate the bunched electrons is not an important parameter. This is in fact not true. Sufficient voltage must be available to accelerate the bunched electrons through the system before space charge debunching becomes important. Furthermore, if the voltage is too small to move the electrons across the microwave structure in a time short in comparison with the microwave period, transit time effects reduce the coupling impedance R' as $(1/t_r)^2$ (see Appendix).

Even in the absence of transit time problems, R' always increases with voltage, because the structures can be made larger and the microwave-electron coupling increases. Calculations with realistic parameter variations have shown that net power output should increase $\sim P \propto V^{5/2}$. Thus we reach our third scaling result; in optimized systems $P \propto V^{5/2}$. A calculation that leads to this result is shown in section D of Appendix II.

III. EXPERIMENTAL RESULTS

Our experiments have been designed to quantitatively test the theoretical predictions discussed above and to investigate the physical parameters of real systems based upon the picosecond demodulation concept.

A. Results From Biplanar Geometries

In this section are contained the results of a series of experiments on biplanar geometry picosecond demodulation sources. This is not a high efficiency coupler, but is especially well suited for testing many of the basic concepts associated with picosecond demodulation sources. This section will show that the results of these experiments are in good agreement with the prediction of the theory.

For the experiments described in this section a biplanar geometry phototube, shown in Figure 8, was used. The optical pulse train was that of Figure 2, with a pulse width of <10 psec and a pulse repetition frequency of 82 MHz.

We have shown (see Appendix I) that the microwave power in each component n is

$$P_n = i_n^2 R' \tag{8}$$

with

$$R' = \frac{2Z_o a}{b}\left[\frac{1}{\omega t_r}\right]^2 = 40\left[\frac{1}{\omega t_r}\right]^2 \tag{9}$$

at 20 KV and 10 GHz,

$$\left[\frac{1}{\omega t_r}\right]^2 \approx \frac{1}{19}$$

and

$$R' \sim 2\Omega \quad .$$

In our experiment $i_a = 1.3$ma or $i_n = 2i_a = 2.6$ ma. Thus we predict

$$\bar{P}_n = 13\ \mu W$$

or for the components between n = 100 → n = 150

$$\bar{P} = 0.7\ mW$$

$$P_{peak} = 0.7\ Watt \quad .$$

We experimentally observed in a 10 GHz system

$$\bar{P} = 0.3\ mW$$

$$P_{peak} = 0.3\ Watt \quad .$$

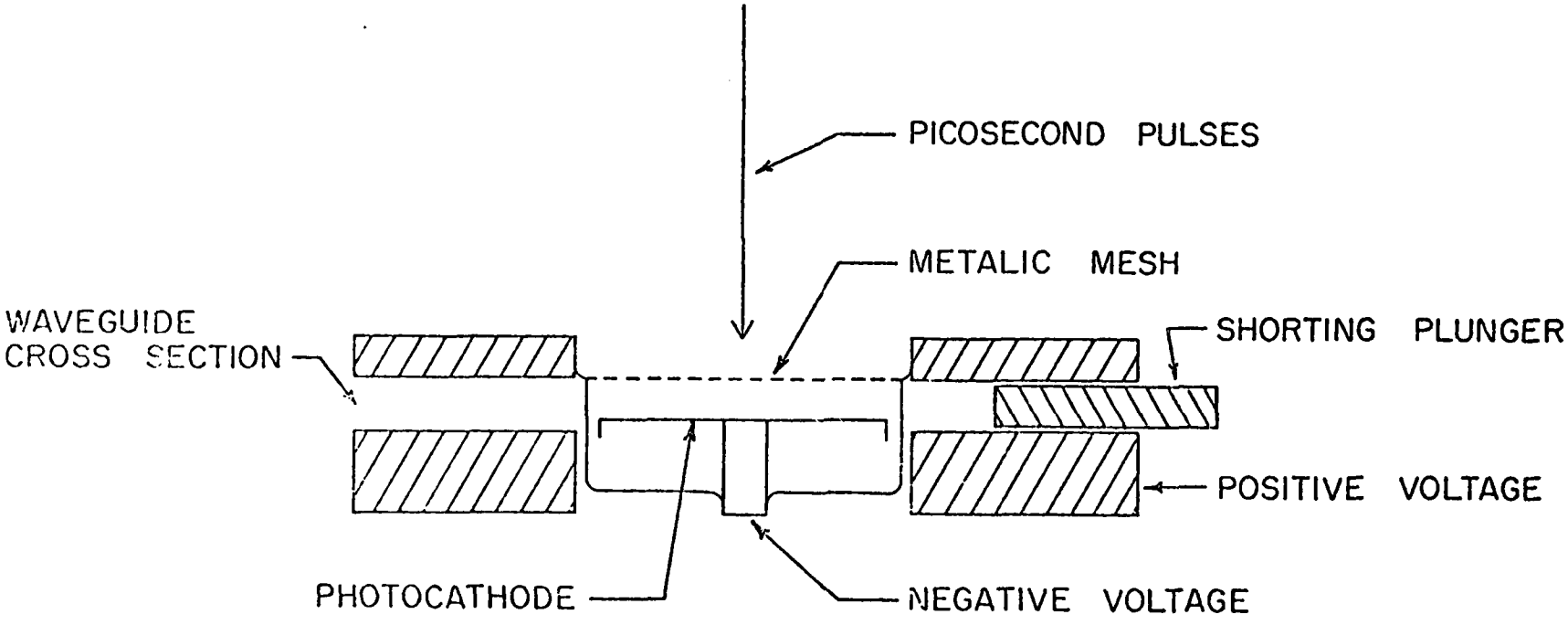

FIGURE 8. BIPLANAR GEOMETRY PICOSECOND DEMODULATION SOURCE.

Because of the $\left(\frac{1}{\omega t_r}\right)^2$ in Eq. 9 , the power output should drop as $(1/\omega)^2$. Below is shown a comparison of our experimental results and theoretical predictions as a function of frequency:

	observed	calculated	obs/cal
(25 GHz)	$\bar{P}$ = .06 mW	.11 mW	.54
	P = .06 Watt	.11 Watt	
(35 GHz)	$\bar{P}$ = .03 mW	.06 mW	.5
	P = .03 Watt	.06 Watt	
(55 GHz)	$\bar{P}$ = .02 mW	.023 mW	.52
	P = .02 Watt	.023 Watt	

Thus we conclude that to within experimental accuracy we have produced the expected microwave power in the 10-55 GHz range. The power fall off is due to transit time limitations which reduce power output by ~x20 at 10 GHz and by ~x600 at 55 GHz. This corresponds to R' (10 GHz) ~ 2Ω, R' (55 GHz) ~ 0.07Ω.

In all of our discussion and calculations to this point, we have assumed that the picosecond pulse length is short in comparison to the microwave period. We have used the same biplaner experimental arrangement to study the relation between the output microwave power and the optical pulse length. Autocorrelation techniques, summarized in Figure 9, were used to measure the length of the picosecond pulse. In our picosecond laser system, the length of the pulse could be conveniently adjusted from ~10 psec to ~40 psec by simply detuning the length of the dye laser cavity. Figure 10 shows the experimental results at 25, 35, and 55 GHz. Figure 11 shows the same results, except that the power output is plotted against the normalized laser pulse length. As expected, the power

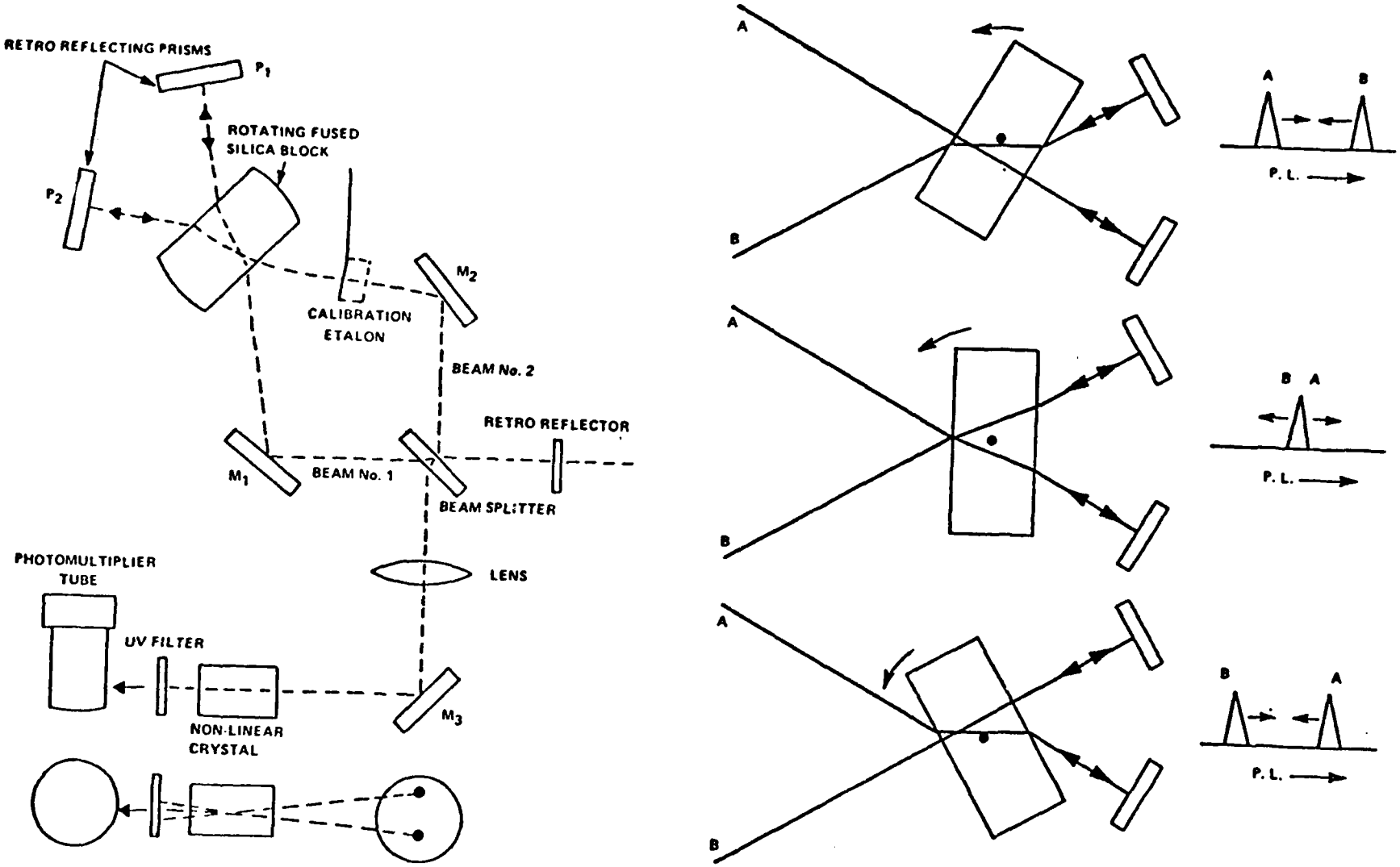

FIGURE 9. AUTOCORRELATION SCHEME FOR MEASURING PICOSECOND PULSE LENGTH.

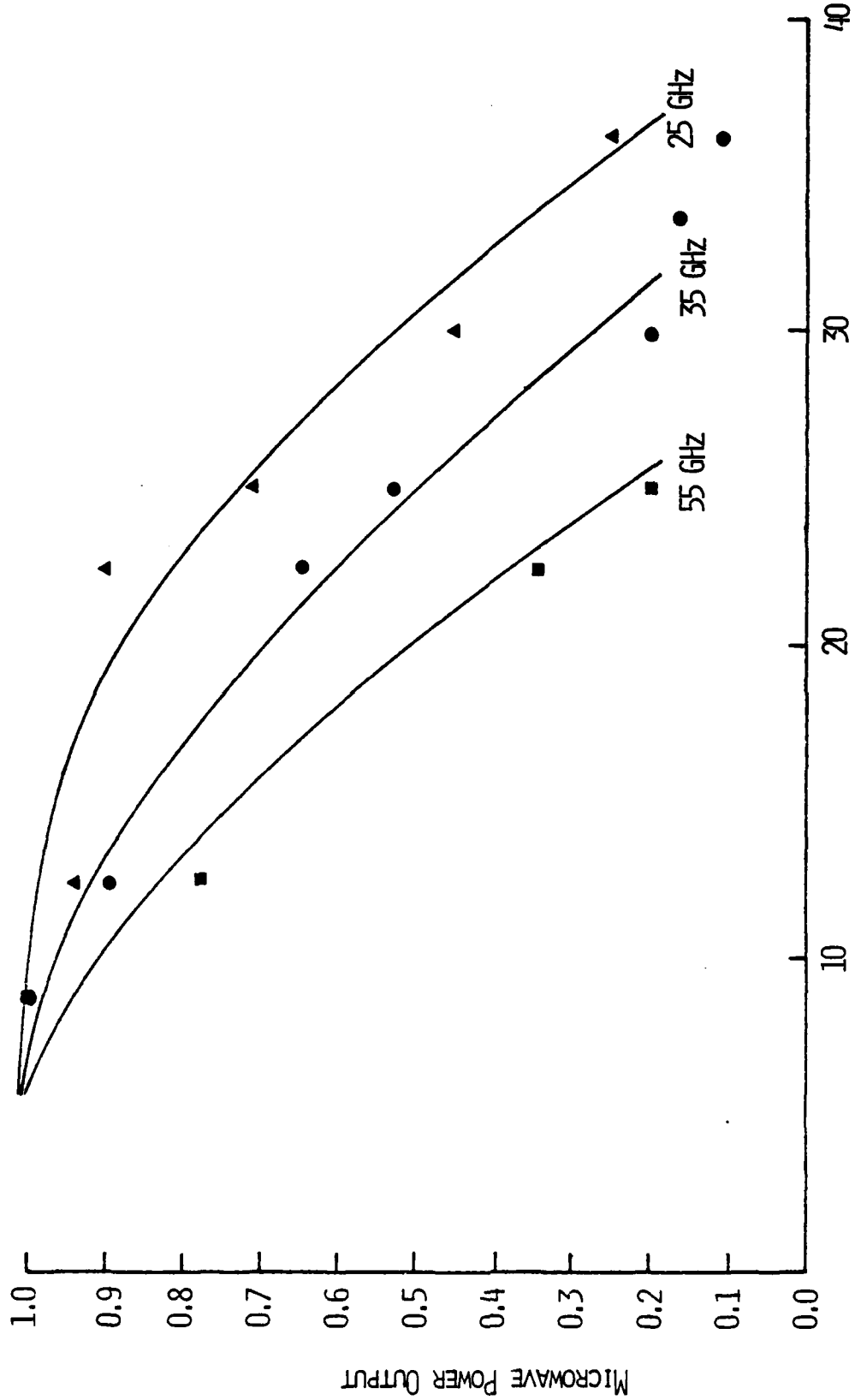

FIGURE 10. MICROWAVE POWER OUTPUT AT 25, 35, AND 55 GHZ AS A FUNCTION OF PICOSECOND PULSE LENGTH.

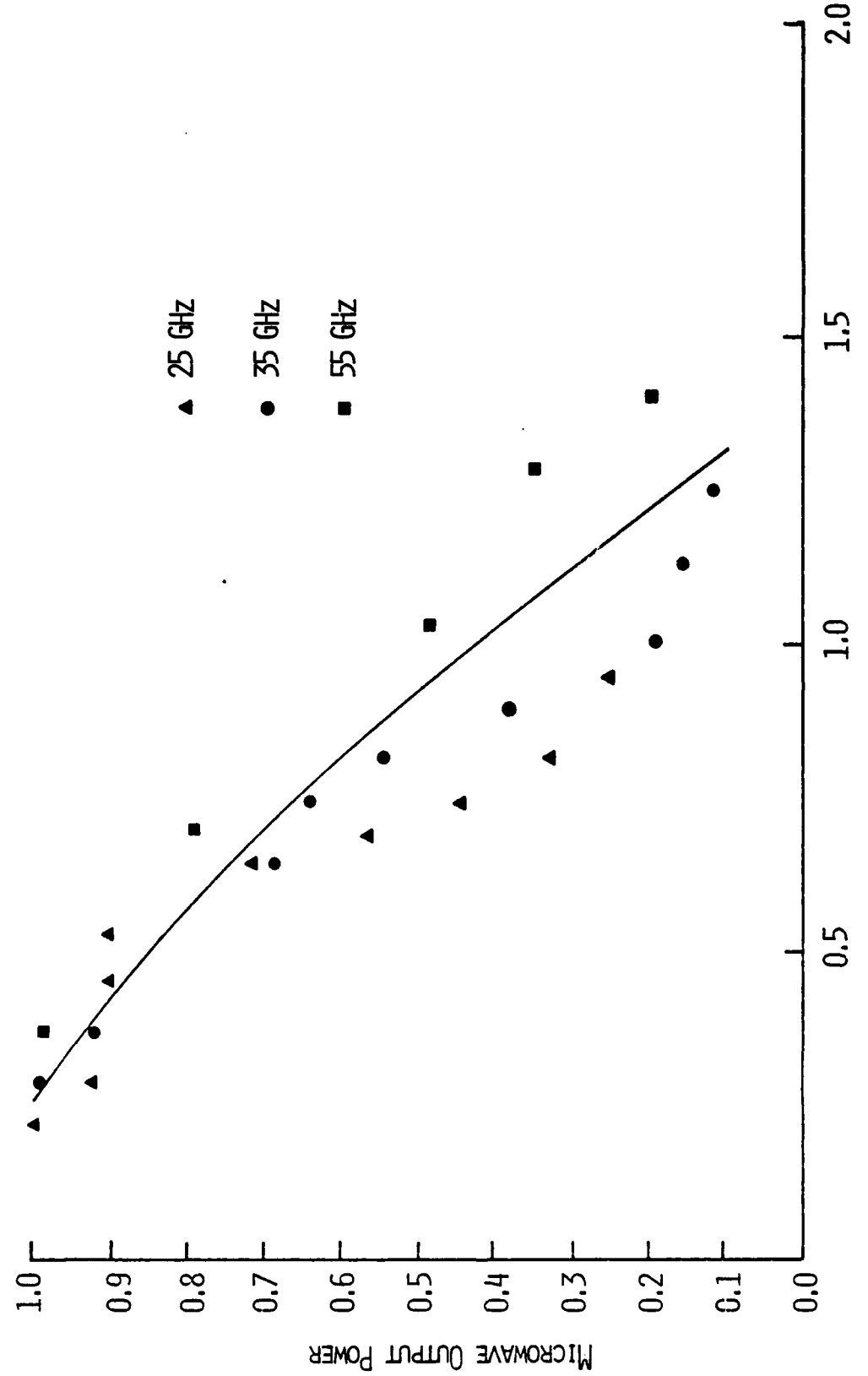

FIGURE 11. MICROWAVE POWER OUTPUT AT 25, 35, AND 55 GHz AS A FUNCTION OF NORMALIZED PICOSECOND PULSE LENGTH.

output decreases with increasing pulse length, with the power output falling to ~0.5 when the optical pulse width is ~.75 of the microwave period. Equation 3 contains the term which predicts the roll off

$$\frac{1}{n} \sin \frac{n\pi\tau}{T}$$

Figure 11 plots the pulse width/microwave period ($n\tau/T$) as the horizontal axis. In the limit that $n\tau/T<<1$ this becomes

$$\frac{\pi\tau}{T}$$

Thus the roll off in power is

$$\left[\frac{\frac{1}{n} \sin \frac{n\pi\tau}{T}}{\frac{\pi\tau}{T}}\right]^2$$

For $(n\tau/T)=0.5$ this factor is 0.81 and for $(n\tau/T)=1.0$ this factor is 0.41. This excellent agreement between experiment and theory must be viewed as at least partially fortuitous because the theory is for rectangular pulses and our experiment uses approximately gaussian pulses. However, this resut is important because it shows that potential problems such as space charge debunching are not substanitally affecting the device.

B. "Snout" Tube Tests of Microwave Interactions

We have designed the tube shown in Figure 12. The idea is that the picosecond bunched electrons can be accelerated by a potential between the grid and cathode and injected into a quartz "snout". Since quartz is a good microwave dielectric, microwave structures can be placed externally to the vacuum, thereby allowing adjustment and refinement of design parameters without requiring a new vacuum encapsuling cycle. First a single reduced height waveguide section (the interaction is essentially the same as the biplanar interaction except that since the electrons are preaccelerated, transit time problems are reduced) was placed around the "snout". This is shown in Figure 13. The microwave output as a function of the location of the microwave structure was investigated and was found to increase slowly as the structure was translated toward the photocathode. Although many effects come into play here, we conclude that the electron bunching remains good down the tube and that wall effects contribute to the changes. When the waveguide structure is converted into a cavity by installing irises, this should increase the coupling resistance R. We observe a X5 increase in output power which is consistent with our expectations for our particular cavity.

Next we designed a "coupled stack" geometry that consisted of 13 reduced height waveguide sections that were coupled together with waveguide. Figure 14 shows this configuration. Figure 15 shows the output of the coupled stack geometry as a function of beam velocity. Phase match (the condition where the electrons travel one period along the microwave structure in one microwave period) occurs at the expected velocity, demonstrating that we can coherently add the output of the individual

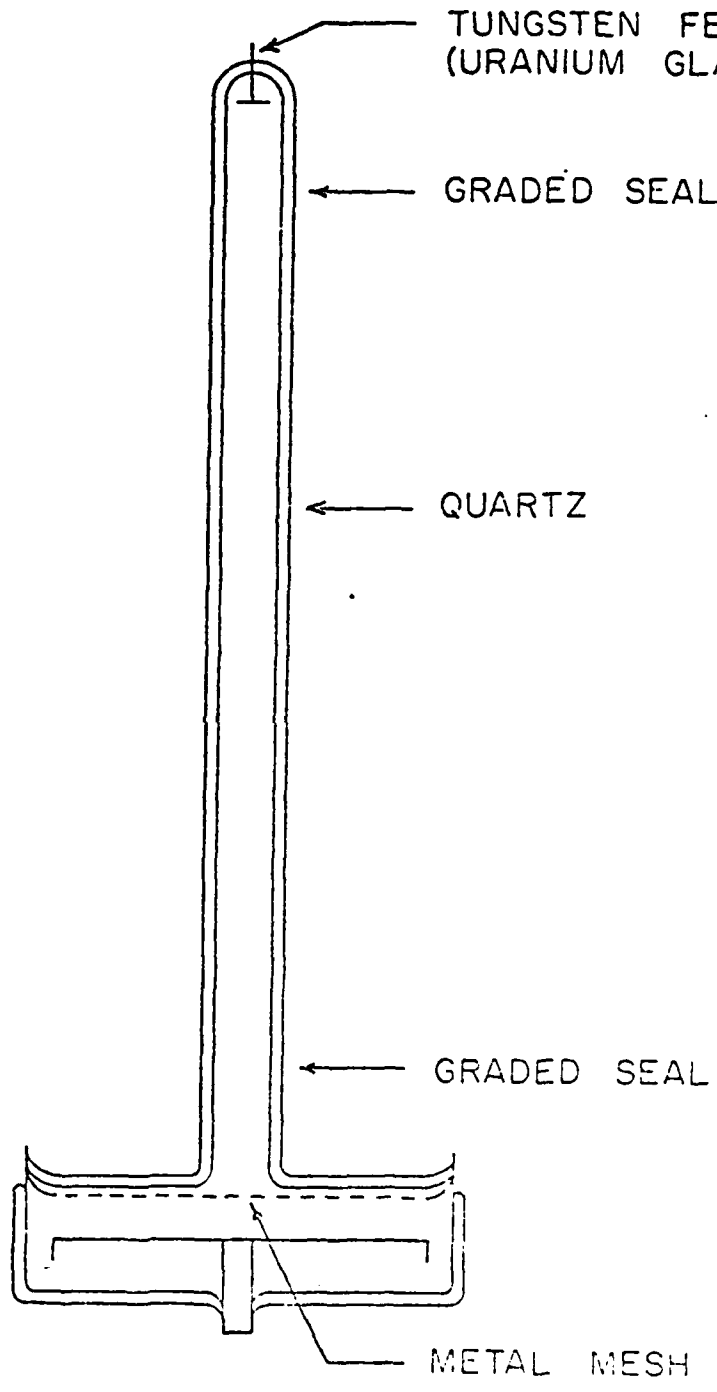

FIGURE 12. "SNOUT" TUBE FOR TESTS OF EXTERNAL MICROWAVE COUPLING GEOMETRIES.

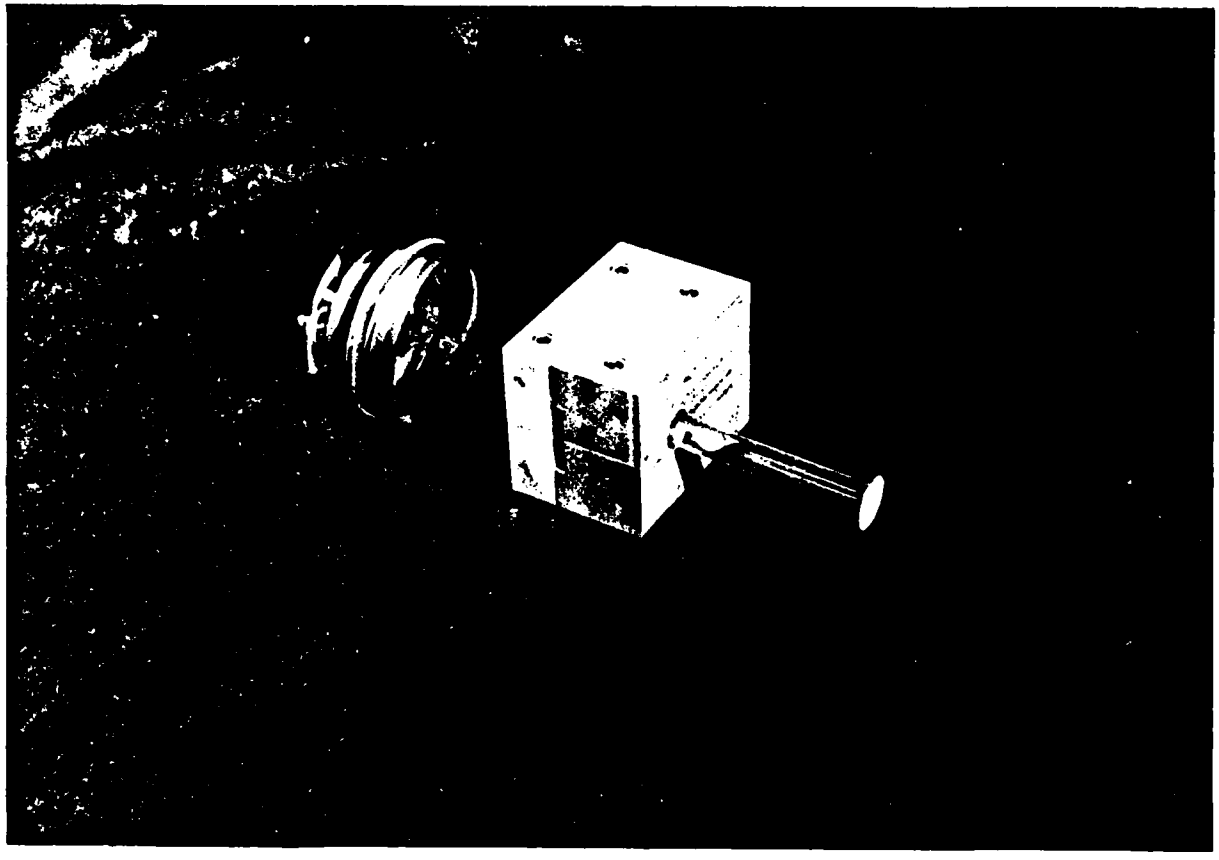

FIGURE 13. "SNOUT" TUBE WITH SINGLE REDUCED HEIGHT WAVEGUIDE STRUCTURE IN PLACE.

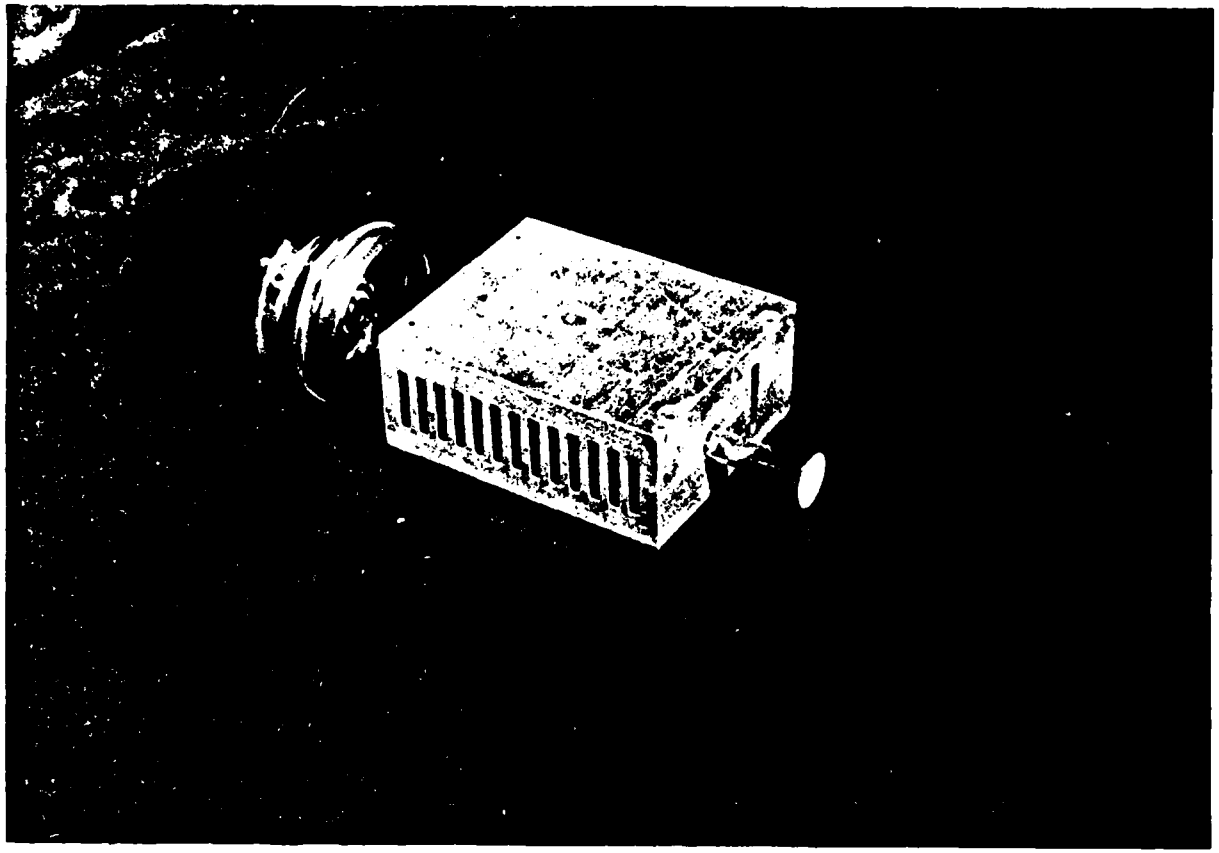

FIGURE 14. "SNOUT" TUBE WITH COUPLED STACK WAVEGUIDE STRUCTURE IN PLACE.

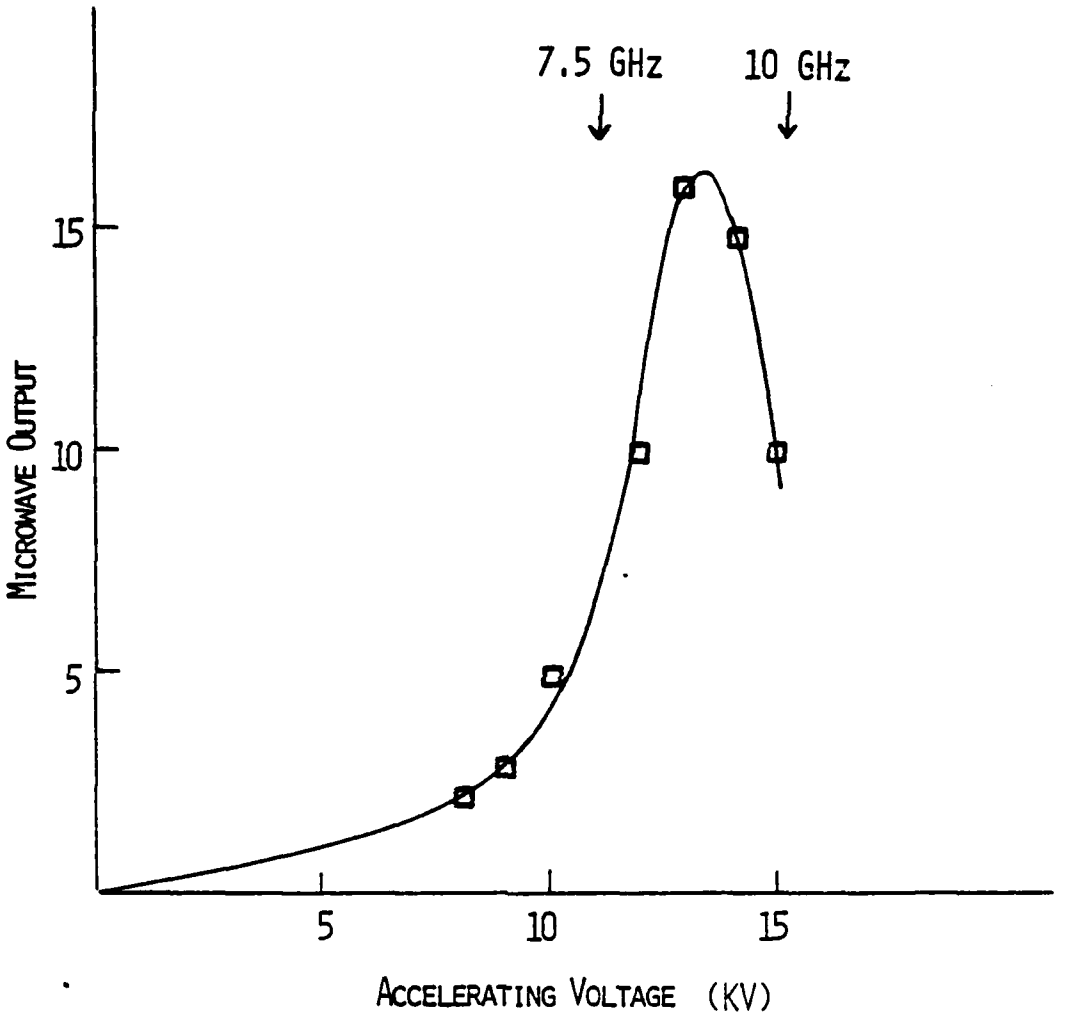

FIGURE 15. OUTPUT POWER AS A FUNCTION OF ACCELERATOR VOLTAGE FOR THE 13 SECTION COUPLED MICROWAVE STRUCTURE.

stack elements. In addition, the power from our coupled stack (13 elements) is observed to be x54 that from a single stack element placed around the snout. The extra x4 comes from the coupling among the elements. The coupling amoung the elements results in a reasonant frequency for this phase match. Thus above the optimum voltage the output decreases.

C. Results from Stack Geometries

Based upon these results we designed two "stack geometry" tubes. These tubes differ from each other in their stack repetition period, being 1/16" and 1/8" respectively. These tubes have been built in our shop and ITT has enclosed them in sealed off vacuum tubes with their photocathodes. Theory predicts that these tubes should produce substantially more power output than the biplanar tubes discussed above, especially at high frequency. This is because the preacceleration of the electrons before the microwave interaction region eliminates the transit time penalty and because a number of interaction regions can be stacked to increase power output. A drawing of this device is shown in Figure 16. Figure 17 shows a photograph of one of these tubes.

Because the accelerating region is separate from the microwave interaction region in the stack geometry tubes, the substantial reduction in R' (and microwave power output, this was a factor of x600 reduction at 55 GHz) theory predicts (and we observe) in the biplanar geometry no longer exists. In addition, the stacking of many microwave interaction regions allows much more power to be coupled out of the electron beam.

Figure 18 shows the results for the stack tube with a 1/8" period structure with a 35 GHz detection system. Since we want the output of the many microwave sources to be in phase, the electron beam velocity must be matched to the period of the structure. The small peak at ~18 KV is probably due to a "subharmonic" (e.g. the electron beam traverses two structure periods in three microwave periods) phasematch. Our results show this "phase match" result and

demonstrate that the microwave output of the several elements can be added coherently. For this system we observe an average power of 10 mW. Since i_n = 900μA, $P = i_n^2 R$ yields (when the contributions of 50 components are allowed for) $R' = 300\Omega$.

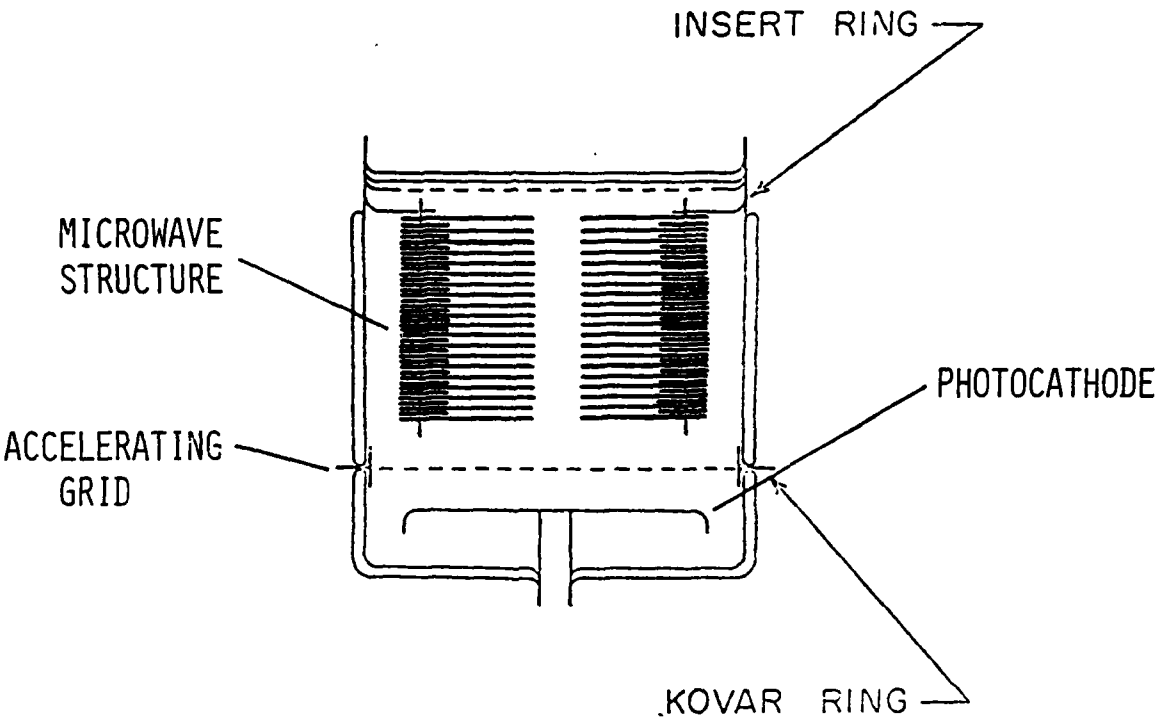

FIGURE 16. SCHEMATIC DRAWING OF "STACK" GEOMETRY TUBE.

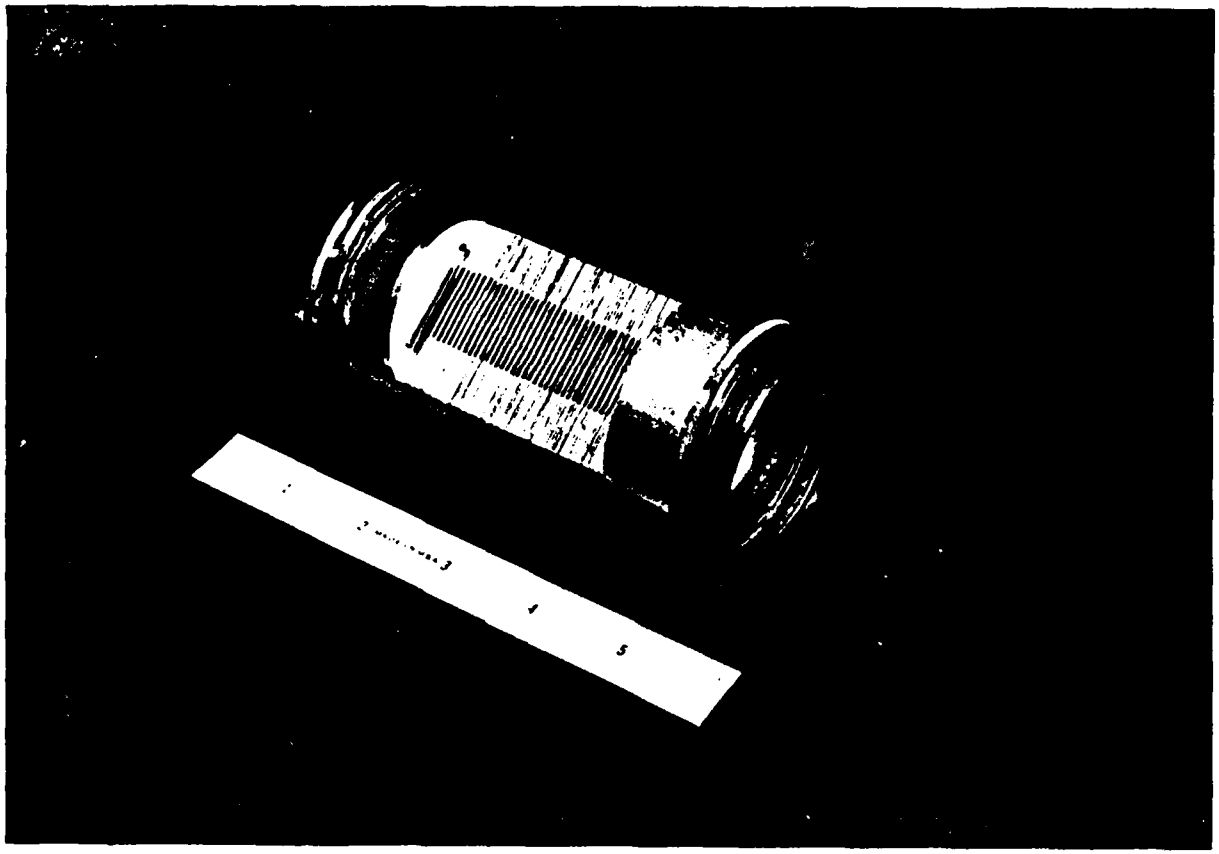

FIGURE 17, STACK GEOMETRY TUBE.

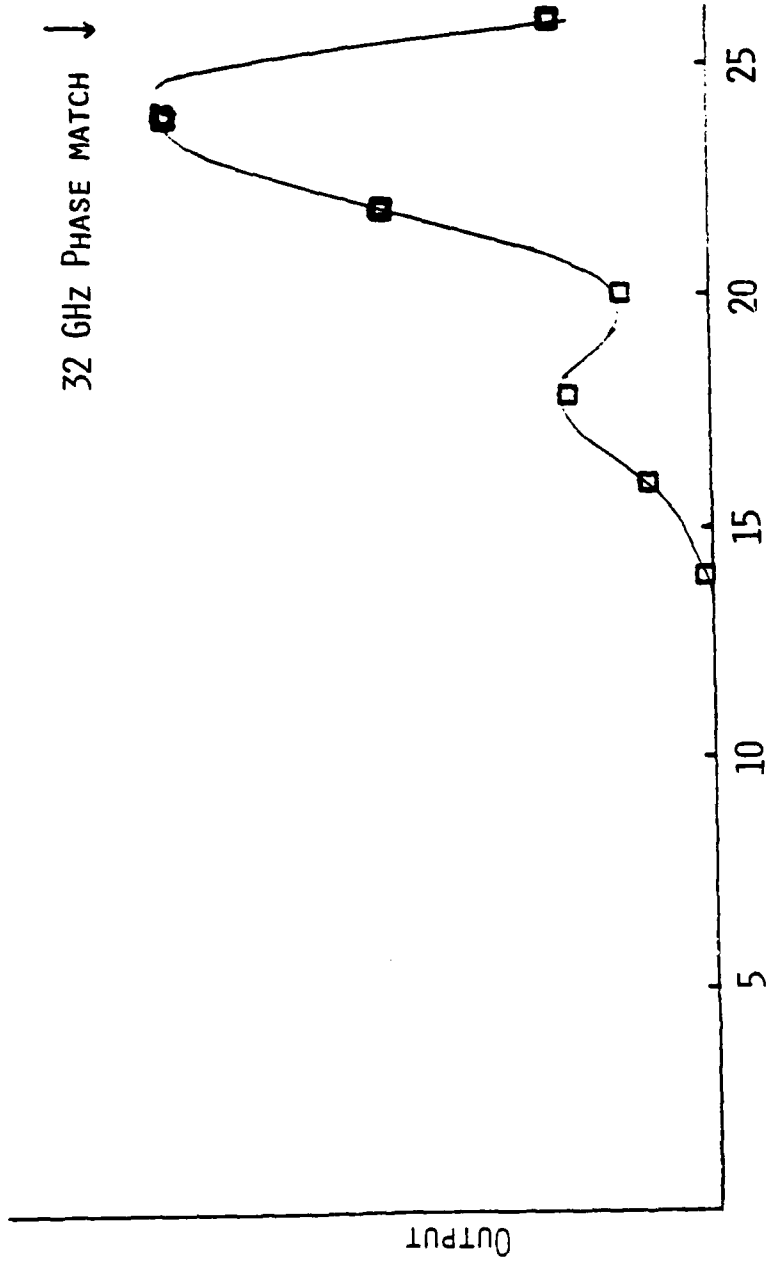

FIGURE 18. 35 GHz output power from the stack geometry tube.

The photocathode in this tube is down by ~x10 from a commercial grade photocathode. Since the scaling law is $P = i^2R'$, this corresponds to 1 W average power. It should be noted that the laser drive power in this case is only 0.1 W. Thus, not only is it demonstrated that the Manley-Rowe criteria does not apply to this class of device (if it did $P_{MW}/P_{laser} < \frac{1}{1000}$), but that conversion gain is possible ($P_{MW}/P_{laser} > 1$). Theory predicts that for a phase matched stack (i.e. no transit time reduction) $R' = \frac{2Z_o a}{b}$, where a is the sum of the heights of the individual elements and b is the width of the slots. For our stacks a/b ~ 2 and so theory predicts $R' = 1200$. Since we do not allow for transmission losses in the pyrex vacuum envelope, etc, this is good agreement. In addition, our 1/16" period stack was used for tests at 55 GHz. This tube has a very poor photocathode in it. With this tube R' ~ 50Ω was observed, but these tests should not be viewed as highly reliable. We have also used these stack tubes to verify the i_a^2 dependence of microwave power. These results are shown in Figure 19, and again we find the agreement to be good. This is an especially stringent test of the i^2 dependence. First, this test is done in the "giant" pulse mode of Figure 5 with a peak current of ~10 A. Secondly, the beam is given substantial distance to debunch as it traverses the length of the stack (~10 cm).

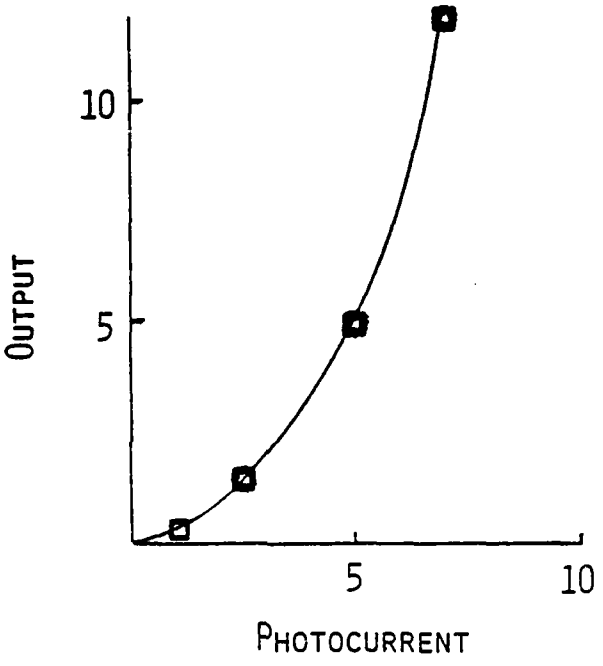

FIGURE 19. SQUARE LAW DEPENDENCE OF MICROWAVE OUTPUT ON PHOTOCURRENT.

D. Coherence and Spectral Purity.

By the very nature of the oscillation process (i.e. stimulated emission gives photons that are in phase with the stimulation), oscillators extract energy from their driving medium coherently (of course an oscillator can still be very unstable). On the other hand, the devices described here are demodulators and their spectral purity and coherence will depend upon the paramters of the driving source. Although there are many ways to approach this issue, perhaps the easiest is to simply note that any variation in the time between the picosecond pulses leads to spectral broadening.

We have investigated this by inspecting the output of our picosecond demodulation sources with a spectrum analyzer. As should be expected, the observed microwave signal was spectually pure (to within the resolution of the available spectrum analyzer, ~1 MHz) as long as the picosecond laser was solidly mode locked. However, detuning one of the adjustments (e.g. the radio frequency drive field) not only caused the microwave frequency to change slightly, but too large a detuning caused the output to become spectually noisy as the mode-lock process deteriorated.

A different kind of test for spectral purity results from our work with the coupled stack. A coupled stack of "n" elements will only produce x"n" power if each of the elements is an incoherent source. However, as noted above we observed about four times this amount.

E. Design and Construction of Second Generation Tubes

Based upon the results of the experiments described above, we have designed and our shop has constructed a second generation of tubes. Figure 20 shows the microwave structure of one of these tubes. This structure is basically a stack geometry with each of the four sides having a different spatial period to phase match different frequencies (up to 220 GHz). In addition, there exists on each side a coupled stack similar to that tested with the snout tube. This coupling between adjacent stack elements should further increase R'.

Figure 21 shows the magnetic resonance structure. This structure is for the investigation of the cycloid resonance configuration discussed in Appendix II.

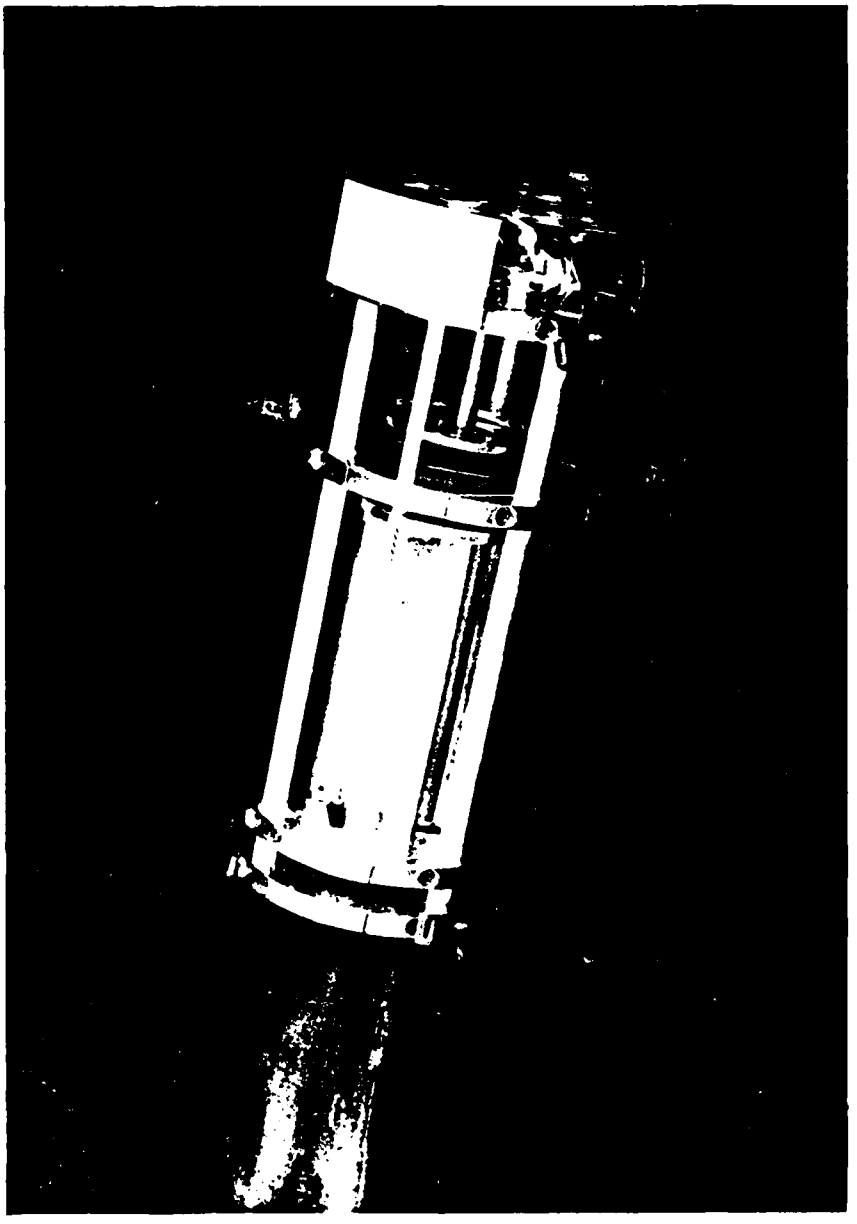

FIGURE 20. SECOND GENERATION STACK GEOMETRY TUBE.

FIGURE 21. FABRY-PEROT CYCLOID TRAJECTORY TUBE.

F. Scaling Laws

We have not been able to test these devices because the photocathodes installed by ITT have been dead. So at this point we will attempt to assess critical issues associated with frequency, voltage and current scaling.

1. High current limits

We have developed the relation $P_{MW} = i_n^2 R'$ and shown it to hold over the range of currents currently available to us. However, commercial, state-of-the-art photocathodes would raise i by x10 and "pulse" laser sources would rise i by several more orders of magnitude. It is reasonable to ask how long this square law increase could be expected to hold. The principal problem should be space charge debunching (thermal effects are more closely related to average current). It should be noted that in our current "giant pulse" configuration (i.e. Figure 5), our single giant pulses correspond to i = 10A. Our i_n is low only because the duty cycle of these "giant pulses" is low. If we only assume that from a solid state laser system we produce "quasi-cw" (i.e. "cw" over the 50 nsec pulse) currents of 10A (i.e. the peak current used in our experiments), equation A.12 yields (with a conservative $R' = 100$) $P = 10^4$ Watts.

2. High voltage regime

As we have discussed earlier, increasing the beam voltage allows an increase in size of the microwave coupling structure. This increase not only reduces fabrication and alignment problems but also increases the area in which electron beam coupling to the microwave structure is efficient. The net effect of this is that

if we keep a particular size structure and operate it at higher frequency by increasing the voltage to continue to meet the phase match condition, R' should remain approximately constant. Thus, even our current 1/16" period 55 GHz stack geometry structure could be operated at 220 GHz by increasing the total accelerating voltage by x16 to ~250 KV. While this is a reasonably high voltage, it must be remembered that no regulation or modulation of this is required and that very simple power supplies are appropriate. It should also be noted that this voltage is applied across the preacceleration gap, not the small microwave structure. A 1/32" period structure would require ~60 KV.

3. High frequency properties

All of our work to date has been done with structures appropriate for the 10-55 GHz region. As shown above, our results have agreed within reasonable experimental error limits with those predicted theoretically. However, it is well known that tubes deteriorate rapidly with increasing frequency and some deterioration should be expected as we move to higher frequencies. However, our current results were achieved by use of very simple and relatively large structures. We also used no guiding $\vec{B}$ field on our beam and no electric focusing. It may well be that more sophisticated manufacturing techniques than our will be required to produce good 220 GHz results, but we are currently far from any practical limits. The principle reason that we have been able to use these simple techniques is that we can use relatively large structures (because of our higher voltages) and because these structures can be simple because we do not require feedback bunching.

IV. POTENTIAL SYSTEM

In this section we will investigate the properties of a picosecond demodulation source based upon a commercial phosphate glass picosecond laser.

A. Solid State Picosecond Lasers

The system used as a baseline is the Quantel PG40 mode-locked phosphate glass system. This system provides ~5 mJ at 1064 nm at a 1 Hz rate. This 5 mJ is distributed among ~10 pulses of duration <10 psec separated by the optical cavity turn around time. I have had a telephone conversation with Kazuko Enterprises, Inc. of Orlando, Florida about the potential use of their compact "mini-range-finder" systems for this application. Their current systems are not mode-locked, but they tell me that there is no reason that they could not be. They point out that because of the short cavity, the mode-lock frequency would be quite high and that they would suggest passive mode-locking to avoid the "high-speed" (~1 GHz) electronics necessary for active mode-locking. Although I am not an expert in mode-locking, 1 GHz is hardly a difficult frequency to work with and I believe that active mode-locking is a viable alternative. According to our conversations, the power and pulse characteristics of the "mini-range-finder" system would not be terribly different from the Quantel System, so the existing Quantel PG40 parameters will be used.

B. A Picosecond Demodulation System

If the 5 mJ of the Quantel PG40 is redistributed by optical techniques into a "cw-like" pulse train of duration 50 nsec, and optical power of 10^5 Watts results. With 10% conversion to second

harmonic and photocathode sensitivity of 50 ma/W, i = 500 A. If a stack geometry provided $R' = 100\ \Omega$, $P = i^2R$ gives 25×10^6 W. This is clearly an unreasonable number. However, if we limit the current 10A, $P = 10^4$ W. In many ways this is a conservative number. Our experiments have been done primarily in the "giant" pulse mode of Figure 5. In this mode, $i_{peak} \simeq 10A$ and we see no evidence of current saturation or space charge debunching. Even with simple microwave structures we have achieved $R' > 100\ \Omega$.

The configuration of this system is shown below. Items (1) through (7) are parts of the Quantel PG40 picosecond laser system. The optical encoder is shown in more detail in Figure 4 of this report and discussed on pages 7-9. In the calculation above $R' = 100\Omega$ was used. As shown in Section III. C, this value of R' can be achieved with relatively simple stack geometrics. It should be possible to achieve much higher R''s with resonant structures (see Section III. B and Appendix II), but some of these are narrow banded and would place constraints upon the frequency agility of the picosecond demodulation sources. The power calculated here is much larger than that achieved with the picosecond demodulation sources driven with the picosecond dye lasers because of the differences in their duty cycles. The general principle is discussed on page 12 of this report. In the specific case discussed here, 10A represents the quasi-cw (i.e. over many NMMW periods) average current. In the dye laser case 10A represents the peak current, but i_n is reduced by ~1000, because the pulse train is as shown in Figure 2. These calculations are wavelength independent. However, as discussed in III. F, large R''s become more difficult with increasing frequency.

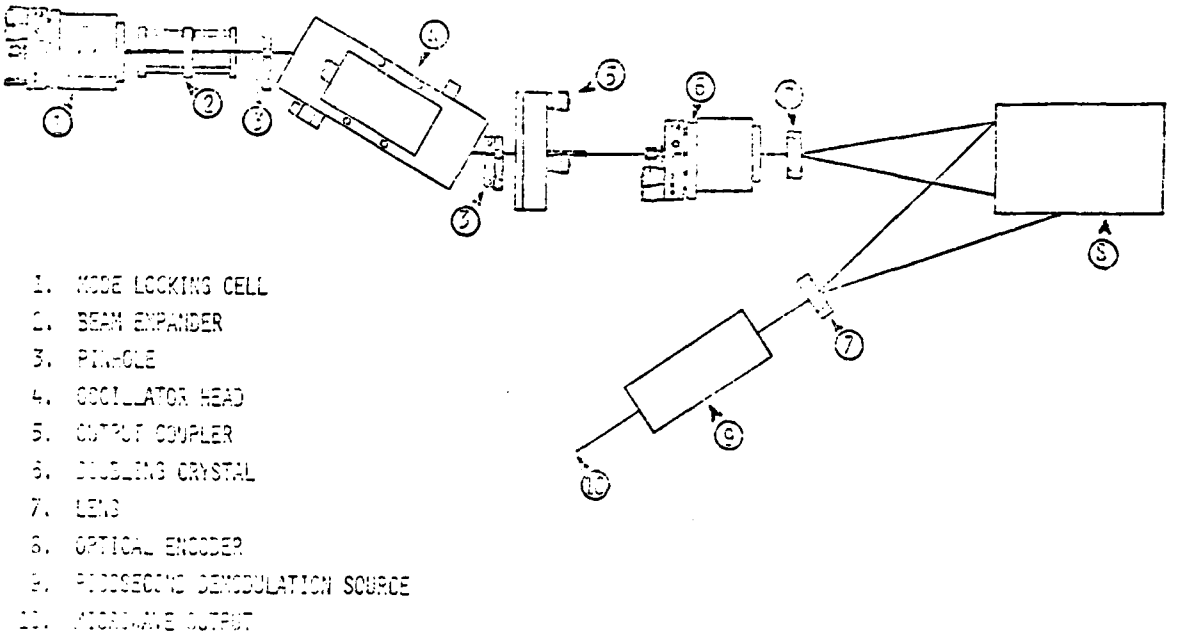

FIGURE 22. SYSTEM BASED ON A PICOSECOND DEMODULATION SOURCE.

In this system the major complexity/cost resides in the picosecond laser. If the system is actively mode locked, the output frequency is directly related to the radio frequency source that drives the mode locker and pulse to pulse phase coherence results. If the laser is passively mode locked, the frequency is determined by the length of the laser cavity, but each pulse has random phase in relation to other pulses. Highly regulated power is not required for the tube because the frequency stability and pulse characteristics come from the laser. No modulator/pulser is required either. Current commercial picosecond lasers are reasonably large and costly. However, laser technology in general and picosecond technology in particular are advancing rapidly as evidenced by devices like minirange finders and GaAs picosecond lasers.

C. A Comparison With Microwave Tubes

In the evaluation of any concept, it is usefult to compare it with alternatives, especially those alternatives that share as many of the same physical attributes and limitations as possible. In this case, an appropriate comparison is with existing microwave tubes. Both tubes and picosecond demodulation devices depend upon the interaction of electron beams with microwave structures. Clearly some of the same principles that limit tubes should also limit these devices. However, classical tubes are constrained to geometries that can provide feedback bunching. In addition, one of the limiting constraints in microwave tubes is the current density available from cathodes. In picosecond demodulation sources, the number of available photoelectrons is very high. For example, in our "giant-pulse" mode, we produce photocurrents of 10A from cathode areas of $<<0.1$ cm^2. This corresponds to current densitities of $>>100$ A/cm^2. This is to be compared with a 5-10 A/cm^2 limit for thermionic impregnated cathodes if reasonable life is required. Perhaps, more importantly, are the power scaling laws with voltage. Although, one can assume that different parameters are held constant and get different results,

$$P \propto V^{5/2}$$

is not unreasonable. This result is closely related to the many "free electron lasers" discussed today; they are in may ways simply high voltage tubes. These devices make it abundantly clear that copious amounts of NMMW energy can be produced if one is willing to go to a high enough voltage acceleration. It can be argued that

~100 kV picosecond demodulation devices represent a technologically interesting ground. 100 KV is easy and cheap to get if you do not require voltage regulation (our devices are not voltage tunable, the frequency comes from the mode-locking/optical pulse train).

The figure below shows the basic configuration for a microwave tube source. In this system a major complexity/ size/cost factor

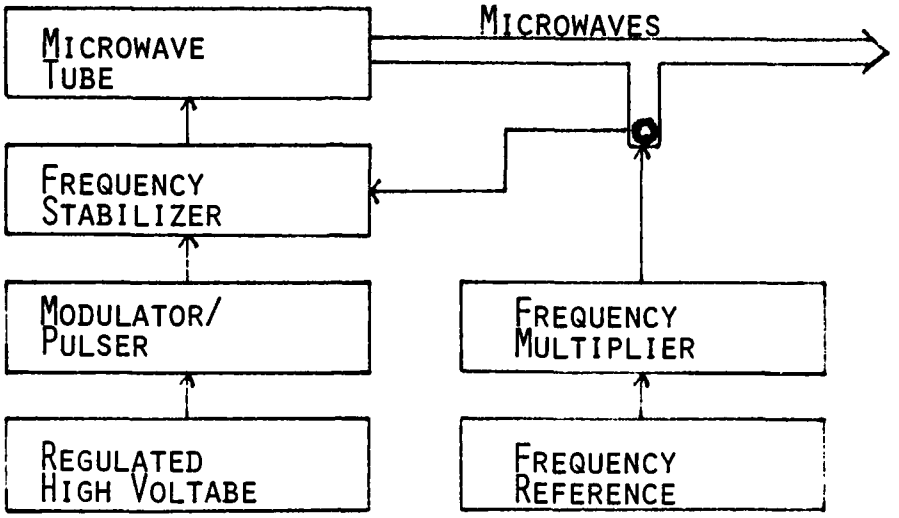

FIGURE 23. SYSTEM BASED ON CLASSICAL TUBE.

resides in the regulated power supply for the microwave tube, the frequency lock loop required for frequency control, and the modulator/pulser. It is possible that the size/cost of such a system could be reduced by the use of a low level driver followed by an amplifier.

Although it would appear that it could be argued that the "ultimate package" based on either of these approaches is better than the other, I think that it is conservative to say that at a minimum the picosecond demodulation approach is an interesting alternative. This is especially true in the environment of rapid technological advance in laser science and the extreme flexibility of waveform generation afforded by the picosecond demodulation system.

D. Technology advances that would be important for systems implementation of picosecond demodulation sources.

1. Laser Development: As discussed above the properties of picosecond demodulation sources are intimately tied to the properties of the drive laser. Although I have not investigated this extensively, developments based upon GaAs picosecond laser (Ap. Aphy. Lett. 39, 525 (1981)) and "mini-rangefinder" type solid state systems seem attractive. Experimental investigation of the limits of the extrapolations in Section III. F. would be important.

2. Electron Multiplier Tubes: The physical process that leads to photomultiplier tubes is fast compared to NMMW time scales. Thus it should be possible to reduce the required picosecond laser power levels by use of electron multiplication techniques. Although the velocity spread of the ejected electrons is a potential problem, photomultipliers whose transit time spread is $< 10^{-11}$ sec have been demonstrated. It is possible to envision a small mode locked solid state laser driving an electron multiplier picosecond demodulation source to very high energy levels.

3. Photocathodes: I am not an expert, but I am concerned about the long term stability of cesium, etc. photocathodes. The ITT people tell me that anti-positive ion emission coatings exist that either eliminate or reduce these problems. One advantage of high peak power laser sources is that efficient x2, x3 multipliers exist that should allow the use of stable photocathodes. The existance (development?) of IR photocathodes for use with GaAs diode lasers or solid state lasers would be interesting.

4. Electron Beam Focusing/Control: All of our current experiments have been carried out without guiding or focusing magnetic or electric fields. Even though we have not encountered any substantial problems because of this, it would appear inevitable that at the highest frequencies these techniques will be required for efficiency. This is an area of substantial commercial expertise both from classical tube design and from the very substantial effort recently on free electron lasers and gyrotrons.

V. SUMMARY

In this work we have demonstrated that picosecond demodulation sources are viable and interesting sources of millimeter wave radiation. The most important attributes of these sources are directly related to the fact that their frequency and amplitude pulse characteristics are determined by simple optical devices rather than by feedback bunching as in a conventional electron beam oscillator. The first of these attributes is the ability of these systems to generate a wide variety of complex microwave waveforms and pulse sequences. The second is that these devices can operate with good spectral purity in the very high voltage regime with very simple, unregulated power supplies.

A theory that relates absolute power output to photocathode current, transit time and accelerating voltage, and microwave structure parameters has been developed and shown to be in good agreement with out experimental results. Scaling laws to higher voltages, higher currents, and higher frequencies have been developed in the context of this theory. On the basis of these experimental and theoretical results, we have proposed a system based upon a picosecond solid state laser.

IV. ACKNOWLEDGEMENT

We would like to express our appreciation to the technical staff of the Electro-Optical Products Division Tube and Sensor Laboratory of International Telephone and Telegraph Corporation, Fort Wayne, Indiana for their assistance in producing the tubes used in this work.

APPENDIX I

The coupling of bunched electron beams to microwave structures.

A. Coupling of bunched electrons to TE_{01} Waveguide Mode

Assume the geometry on the right; the bunched photoelectrons start at the center bottom of guide and are accelerated by V_o to top.

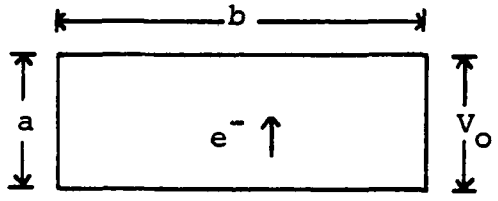

(1) Simple calculations show that the transit time is given by

$$t_r = \left(\frac{2ma^2}{V_o e}\right)^{1/2} \tag{A.1}$$

where V_o is the potential across guide, e is the charge on electron, m is the mass of electron, t_r is the transit time, a is the guide height, and b is the guide width.

(2) Next we calculate the energy given up to the microwave field by a single bunch of charge q

$$W = \int F \cdot dr \tag{A.2}$$

$$F = q \frac{V_1}{a} \cos(\omega t+\phi) \tag{A.3}$$

$$W = q \frac{V_1}{a} \int \cos(\omega t+\phi) dz \tag{A.4}$$

$$W = q \frac{V_1}{a} \int_o^{t_r} \frac{V_o e}{ma} t \cos(\omega t+\phi) dt \tag{A.5}$$

$$W = \frac{q^2 V_1 V_o e}{ma^2} \int_o^{t_r} t \cos(\omega t+\phi) dt \tag{A.6}$$

where $\frac{V_1}{a}\cos(\omega t+\phi)$ is the microwave field. We substitute $x=\omega t+\phi$ to put in integrable form and finally get

$$W = \frac{2eV_1}{\omega^2 t_r^2}\left[\cos(\omega t_r+\phi) + \omega t_r \sin(\omega t_r+\phi) - \cos\right] \qquad (A.7)$$

(3) Next we calculate the power tranferred by a square wave modulated beam of "n" electrons/sec to be

$$P = \frac{2V_1}{\omega^2 t_r^2}\frac{ne}{t}\left[\text{above}\right] = \frac{2V_1 i}{\omega^2 t_r^2}\left[\text{above}\right] \quad . \qquad (A.8)$$

Two limiting cases of this equation should be considered in order to give us results that we need for very nice physical interpretations in part B.

(a) $\omega t_r << 1$; choose $\phi=0$ $\Rightarrow$ $\left[\text{above}\right] = \omega^2 t_r^2$

$$\Rightarrow P = 2iV_1$$

(b) $\omega t_r >> 1$, choose V_o for which $\sin(\omega t_r+\phi) = +1$

$$\Rightarrow \left[\text{above}\right] = \omega t_r$$

$$\Rightarrow P = \frac{2iV_1}{\omega t_r}$$

B. Energy transfer from modulated beam, impedance point of view.

(1) The relationship between the power flow in a waveguide and E field has the general form $P = kE^2$, where k depends on the structure. For TE_{01} waveguide

$$P = \frac{ab}{2Z_o}E^2 = \frac{ab}{2Z_o}\left(\frac{V_1}{a}\right)^2 = \frac{b}{2Z_o a}V_1^2 \qquad (A.9)$$

or $$P = \frac{V_1^2}{R} \qquad (A.10)$$

with $$R = \frac{2Z_o a}{b} \qquad (A.11)$$

where $R \equiv$ effective resistance of structure.

(2) If a current i, modulated at a frequency which the mode structure can support (so it looks like a resistance), flows across the guide

$$P = i^2 R \qquad (A.12)$$

will be put into the MW mode. This assumes

(a) No transit time effects.

(b) That the electron has enough energy to make it across the guide. This is effectively a question of impedance matching; if an accelerating voltage of V_o is applied, the beam impedance becomes

$$Z_b = V_o/i \quad .$$

(3) We must now include transit time effects on effective impedance. In part A we showed for $\omega t_r >> 1$ that

$$P = iV_1/\omega t_r \quad .$$

In part B we showed

$$P = V_1^2/R \quad .$$

Eliminating V_1 yields

$$P = i^2 R/(\omega t_r)^2 = i^2 R' \Rightarrow R' = R/(\omega t_r)^2 \qquad (A.13)$$

where R' is the effective impedance including transit time effects. We conclude that from the point of view of energy transfer from

the beam to the microwave mode that we lose as $(1/t_r)^2$ for $\omega t_r >> 1$.

C. A simple transit time/impedance argument

(1) Assume a guide of dimension a x b and a TE_{01} mode.

(2) Assume that because of transit time considerations that the electron sees "n" phase reversals of the electric field ("n" can always be made to be an integer by adjustment of the accelerating field). Now:

(a) if n is odd => no net output

(b) if n is even => output, but only electron-field interaction after last reversal contributes energy to MW mode.

(3) In a TE_{01} mode $P = \frac{ab}{2Z_o} E^2$. For "n" reversals, the guide can be divided into n + 1 regions, each which has equal power content. The last segment of the guide is equivalent to a guide of height a' = a/(n+1) and power content P' = P/(n+1).

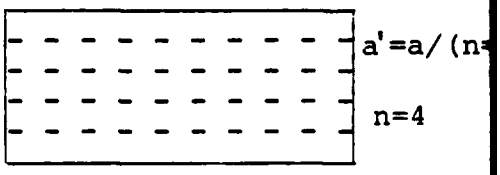

(4) $E = V_1/a$, substituting all primes

$$P/(n+1) = \frac{[a/(n+1)]b}{2Z_o} \left[\frac{V_1}{a/(n+1)}\right]^2 \rightarrow P = \underbrace{\frac{b}{a}\frac{1}{2Z_o}}_{1/R'} (n+1)^2 V_1^2$$

$$R' = \frac{2Z_o a}{b} \frac{1}{(n+1)^2} .$$

(5) Since R' is ordinarily much too low for efficient transfer of energy from beam to waveguide

$$P_t \propto \frac{1}{(n+1)^2} .$$

D. The relation between beam accelerating voltage and power output

This section addresses the question of the role played by the accelerating voltage on output power once this voltage is large enough to eliminate the transit time penalty discussed above. This voltage scaling is clearly model dependent, but we will choose parameters that are appropriate for picosecond demodulation devices and will obtain "standard" results.

Equation A.12 does not contain explicitly any voltage dependence. However, both "i" and "R" depend upon V because in a transit time limited device the size of the microwave structure scales with the voltage. Consider the interaction with a TE_{01} waveguide mode (this is the basic interaction of the stack geometry). If V is increased, the beam velocity increases as $V^{1/2}$, and the height of the structure "a" may also be increased as $V^{1/2}$. This directly increases R as $V^{1/2}$ (see A.11). Furthermore, the effective value of "i" increases as V. This can be seen as follows. The real physical limits are on current density, not current, the major limits being space charge debunching and cathode current density. The area over which an interaction between a microwave structure and the bunched electron beam can take place efficiently is governed by the area occuppied by the fringing microwave field of the structure. As the height of the microwave structure is increased, the linear extent of the fringing field increases in direct proportion, but the area increases as the square. Since the height "a" increases as $V^{1/2}$.

the interaction area increases as V. Thus since $P = i^2R$, the scaling of "i" and "R" with voltage in a transit time limited device, give the resultant voltage scaling law

$$P \propto V^{5/2} \quad . \tag{A.14}$$

APPENDIX II

In this appendix we will briefly discuss the basic concepts associated with high efficiency microwave couplers and discuss several specific couplers. As shown in Appendix I, for a single interaction region of height a, width b, and transit time t_r, $P = i^2R'$, with

$$R' = \frac{2Z_o a}{b}\left(\frac{1}{\omega t_r}\right)^2$$

The physics behind the terms in this equation are straightforward to assess. As "a" is increased the microwave field has longer to interact with the electrons and to extract energy; thus, "a" is in the numerator. However, as "b" is increased, the microwave energy is spread over a greater volume, and the field available to interact with the electron is reduced, thus, "b" is in the denominator. Appendix I discusses the role of transit time. In general, the desire to increase "a" and at the same time decrease t_r are in conflict, but structures that eliminate this problem are possible. An approach to the solution of this problem is the triplanar geometry.

A. TRIPLANAR GEOMETRY: This is the first order extension from the biplanar device that has been tested. By separation of the accelerating region from the interaction region, the transit time term $(1/\omega t_r)^2$, can be reduced to ~1. In our biplanar tests, this effect reduced output by ~ a factor of 20 at 10 GHz and 600 at 55 GHz.

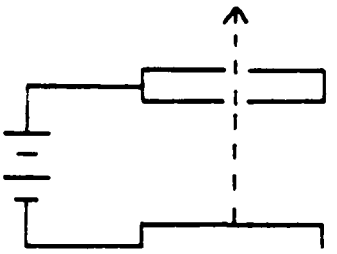

photocathode

ADVANTAGES:

(1) Simple, easy to construct even at 200 GHz

(2) Broadbanded

DISADVANTAGES:

(1) Not really a high efficiency coupler, because even if the electrons are accelerated to a speed approaching c, "a" must be $\lesssim \lambda/2$.

B. STACK GEOMETRY: Conceptually this is very similar to the tri-planar geometry, but by stacking "n" additional interaction regions, we get xn output, n = 100 is reasonable.

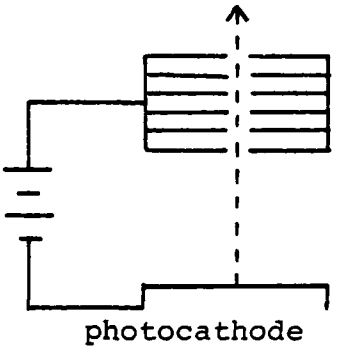

ADAVANTAGES:

(1) Simple, easy to construct geometry even at 200 GHz

(2) Broadbanded

DISADVANTAGES:

(1) Not really optimum use of microwave field to increase coupling efficiency

At this point the optimum use of the microwave field must be discussed. Fundamentally, the microwave field that interacts with the electrons should be as large as possible. All of the geometries to this point allow the microwave energy to propagate away from the interaction region. Geometries that either trap the radiation in a resonant cavity or cause the microwave energy to propagate along the direction of the electron beam are substantially more

efficient. Although an exact calculation depends upon the details of the geometry, a good estimate of the enhancement factor can be obtained by simply noting that the reflectivity of copper is ~99% in this spectral region and that the increase in coupling efficiency is directly proportional to the number of passes that the microwave energy makes through the interaction region. Thus, the coupling efficiencies of the above can be increased by x10 → x100 by converting the waveguide to enclosed cavities or by coupling the elements of the stack together in a traveling wave fashion. The stack geometry would then be a very high efficiency coupler.

C. PRE-ACCELERATED TRAVELING WAVE GEOMETRY: Many variations on this concept exist, only the simplest is shown. This is basically the triplanar geometry stretched to include many discreet photocathodes. In this geometry, "phased arrays" are "constructed" on a large area photocathode by optical techniques. This is one means of generating complex microwave pulse sequences. In addition, the average current density on the photocathode is reduced. This could be important if very large optical pulses were used. This geometry is also adaptable to stack geometries.

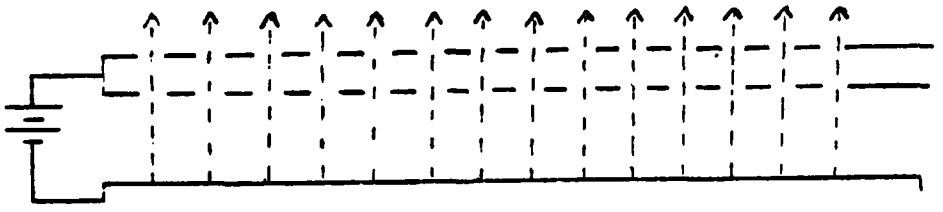

photocathode

Magnetic fields can also be used to overcome the conflict between the desire for a long interaction time and transit time problems. In these approaches the cyclotron (or cycloid) motion of electrons in magnetic fields is used to introduce a periodicity into the interaction. Unfortunately, a magnetic field of the order of 100 kG is required to produce a cyclotron frequency of 220 GHz. Fortunately, rather efficient coupling on harmonics of the cyclotron frequency is possible. This is because at the lower fields appropriate for subharmonic operation, the cycloid trajectories are larger and they move more efficiently from high field regions to low field regions in the cavity.

D. CYCLOID TRAJECTORIES IN FABRY-PEROT CAVITY: If one plate of a Fabry-Perot cavity is the photocathode, the anode the other plate, and a magnetic field is applied perpendicular to the axis of the cavity, the motion of ejected electrons is described by a cycloid. If the period of this cycloid is the same as the period of the cavity (or some subharmonic) efficient coupling of the bunched electrons to the cavity mode results.

ADVANTAGES:

(1) The cavity produces a high microwave field and a correspondingly high coupling efficiency.

(2) The electrons interact with the field for many cycles.

(3) The cycloid motion can be executed by an entire sheet of electrons. This means that space charge debunching is minimized.

(4) No small dimentions.

DISADVANTAGES:

(1) Requires a magnetic field.

(2) It is narrow banded (but tunable) because of the cavity.

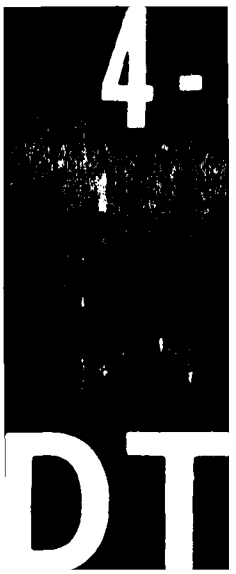
4-
DT